FINITE TYPE INVARIANTS OF W-KNOTTED OBJECTS III: W-FOAMS, THE KASHIWARA-VERGNE THEOREM AND DRINFEL'D ASSOCIATORS

DROR BAR-NATAN AND ZSUZSANNA DANCSO

ABSTRACT. This is the third in a series of papers studying the finite type invariants of w-knotted objects and their relationship to the Kashiwara-Vergne problem and Drinfel'd associators. In this paper we present a topological solution to the Kashiwara-Vergne problem. In particular we recover via a topological argument the Alkeseev–Enriquez–Torossian [AET] formula for explicit solutions of the Kashiwara-Vergne equations in terms of associators.

The w-knotted objects at the centre of this paper, *w-foams*, are knottings of 2-dimensional surfaces and associated features in four-dimensional space. We use a topological construction – which we name the double tree construction – to show that every *homomorphic expansion* (or *formality isomorphism*) of parenthesized braids extends first to an expansion of knotted trivalent graphs (a well known result), and then uniquely to an expansion of w-foams.

In algebra, a homomorphic expansion for parenthesized braids is uniquely determined by *Drinfel'd associator* Φ, and a homomorphic expansion for w-foams is uniquely determined by a solution V of the Kashiwara-Vergne problem [KV], as reformulated by Alekseev and Torossian [AT]. Hence our construction provides a topological framework and independent topological proof for the Kashiwara–Vergne Theorem, and the [AET] formula.

CONTENTS

1. Introduction

1.1. Executive Summary.

This brief section is a large-scale overview of the main result of this paper and the idea behind its proof; it is followed by a detailed introduction.

A *homomorphic expansion* for a class of topological objects $\mathcal{K}$ is an invariant $Z\colon \mathcal{K} \to \mathcal{A}$ whose target space $\mathcal{A}$ is canonically associated with $\mathcal{K}$ (its *associated graded structure*). Homomorphic expansions satisfy a certain universality property, and respect operations which exist on $\mathcal{K}$ and therefore also on $\mathcal{A}$. Such invariants are often hard to find, and when they are found, they are often deeply connected with quantum algebra and/or Lie theory:

- For many classes of knotted objects in 3-dimensional spaces homomorphic expansions don't exist — for example, one would have loved ordinary tangles to have expansions compatible with disjoint unions and tangle compositions, but they don't.
- Yet *parenthesized tangles*, or, nearly-equivalently, *knotted trivalent graphs* in $\mathbb{R}^3$ – which, for the purpose of this short summary, denoted $\mathcal{K}^u$ here, and *sKTG* later – do have homomorphic expansions. A homomorphic expansion $Z^u\colon \mathcal{K}^u \to \mathcal{A}^u$ is defined by its values on a couple of elements of $\mathcal{K}^u$ which generate $\mathcal{K}^u$ using the operations $\mathcal{K}^u$ is equipped with. The most interesting of these generators is the tetrahedron $\triangle$. Importantly, $\Phi = Z^u(\triangle)$ turns out to be equivalent to a *Drinfel'd associator*.
- A certain class of four-dimensional knotted graphs called *w-foams* – denoted $\mathcal{K}^w$ for now, *wTF^o* later in the paper – also has homomorphic expansions. The most interesting generator of $\mathcal{K}^w$ is the *vertex* $\curlywedge$, and if $Z^w\colon \mathcal{K}^w \to \mathcal{A}^w$ is a homomorphic expansion, then $V = Z^w(\curlywedge)$ is equivalent to a solution of the *Kashiwara-Vergne problem* in Lie theory.

Roughly speaking, $\mathcal{K}^u$ is a part of $\mathcal{K}^w$ and $\mathcal{A}^u$ is a part of $\mathcal{A}^w$, as in the figure on the right. More precisely, there are natural maps $a\colon \mathcal{K}^u \to \mathcal{K}^w$ and $\alpha\colon \mathcal{A}^u \to \mathcal{A}^w$. The main purpose of this paper is to prove the following theorem, whose precise version is stated later as Theorem 1.2:
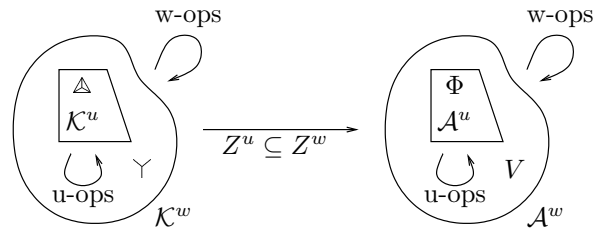
Main Theorem. Any homomorphic expansion Z^u for $\mathcal{K}^u$ extends uniquely to a homomorphic expansion Z^w for $\mathcal{K}^w$, and therefore, any Drinfel'd associator Φ gives rise to a solution V of the Kashiwara-Vergne problem.

The proof of this theorem is conceptually simple: we show that the generators of $\mathcal{K}^w$ can be explicitly expressed using the generators of $\mathcal{K}^u$ and the operations of $\mathcal{K}^w$, and that the

resulting explicit formulas for $Z^w(\curlywedge)$ (and for Z^w of the other generators) satisfy all the required relations.

The devil is in the details. It is in fact impossible to express the generators of $\mathcal{K}^w$ in terms of the generators of $\mathcal{K}^u$ — to do that, one first has to pass to a larger space $\tilde{\mathcal{K}}^w$ (in the paper $\widetilde{wTF}$), which has more objects and more operations, and in which the desired explicit expressions do exist. But even in $\tilde{\mathcal{K}}^w$ these expressions are complicated, and in order to verify the relations they need to be expressed using the framework of a multi-step "double tree construction". A brief pictorial summary of the construction is below, and the explanation takes up the bulk of this paper:
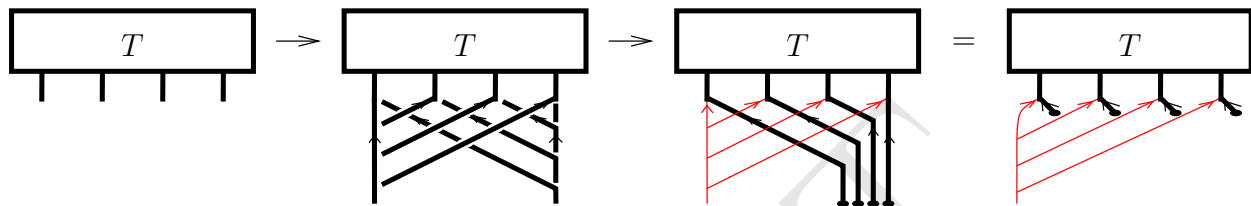
1.2. **Detailed Introduction.** This paper is the third in a sequence [WKO1, WKO2, WKO3] studying finite type invariants of w-knotted objects, and contains the strongest result: a topological construction for a homomorphic expansion of *w-foams* from the Kontsevich integral. This in particular implies the Kashiwara-Vergne Theorem of Lie theory, more precisely, it gives the [AET] formula for solutions of the Kashiwara-Vergne equations in terms of Drinfel'd associators.

The papers in this sequence need not be read consecutively. Readers broadly familiar with finite type invariants will have no trouble reading [WKO2] and this paper without having read [WKO1]. However, the setup and main results of [WKO2] are used heavily in this paper. Reproducing all necessary details would be lengthy, but we include concise summaries for readers already familiar with the content, and otherwise refer to specific results or sections of [WKO2] throughout.

The Kashiwara-Vergne problem — KV problem for short, proposed in 1978 [KV] and proven in 2006 by Alekseev and Meinrenken [AM] — asks whether solutions exist for a certain set of equations in the space of "tangential automorphisms" of the free lie algebra on two generators. For a precise statement see Section 1.2.1. The existence of such solutions has strong implications in Lie theory and harmonic analysis, in particular it implies the multiplicative property of the Duflo isomorphism, which was shown to be knot-theoretic in [BLT, BDS].

In [AT] Alekseev and Torossian gave a proof for the existence of KV solutions based on a deep connection with Drinfel'd associators. In turn, Drinfel'd's theory of associators [Dr] can be interpreted as a theory of well-behaved expansions (universal finite type invariants) of parenthesized tangles[1] [LM, BN2], or of knotted trivalent graphs [Da, BND1]. In [AET] Alekseev, Enriquez and Torossian gave an explicit formula for solutions of the Kashiwara-Vergne equations in terms of Drinfel'd associators.

In [WKO2] we re-interpreted the Kashiwara-Vergne conjecture as the problem of finding a homomorphic expansion of a class of knotted surfaces – *w-foams* – in 4-dimansional space,

---

[1] "q-tangles" in [LM], "non-associative tangles" in [BN2].

and explained the connection to Drinfel'd associators in terms of a relationship between 3-dimensional and 4-dimensional topology. Another topological interpretation for the KV problem in terms of the Goldman-Turaev Lie bialgabra later emerged in [AKKN1, AKKN2], and the papers [M] and [AN] contain constructions of Goldman-Turaev expansions from the Kontsevich integral and the Knizhnik-Zamolodchikov connection, respectively.

The algebraic structure of w-foams is built on the concept of a *circuit algebra*, which was also identified as equivalent to the operadic structure of a *wheeled prop* in [DHR1]. The symmetry groups of Kashiwara-Vergne solutions, called the Kashiwara-Vergne groups, are shown to be automorphism groups of the w-foam circuit algebra and its associated graded arrow diagrams in [DHR2]. The relationship between the symmetries of Drinfel'd associators – the Grothendieck-Teichmuller groups – and the Kashiwara-Vergne groups is described in the topological context of w-foams in [DHoR].

In this paper we present a topological construction for a homomorphic expansion of w-foams, thereby giving a new topological proof for the KV conjecture. This construction also leads to an explicit formula for KV-solutions in terms of Drinfel'd associators, which we prove agrees with the formula [AET, Theorem 4]. Computational verification of these results is given in [WKO4]. We conclude this introduction with a brief review of the KV Problem, a summary of the topological and algebraic tools developed in this paper, and we state the main result.

1.2.1. *The Kashiwara–Vergne Problem.* This section presents a brief review of the Kashiwara-Vergne (KV) equations [AT]. Readers unfamiliar with the subject but interested in the connection between w-foams and the Kashiwara–Vergne problem may refer to [WKO2, Sections 3 and 4] for details, as well as [AT, Sectons 1–5]. Readers interested primarily in the topology may skip this section without much impact.

For a re-cap of basic definitions and notation, let $\mathfrak{lie}_n$ denote the *degree completed* free Lie algebra on n generators $\{x_1, ..., x_n\}$. When n is small, we will denote the generators by x, y, z. Let $\mathfrak{tder}_n$ denote *tangential derivations* of $\mathfrak{lie}_n$, that is, derivations d with the property that $d(x_i) = [x_i, u_i]$, with $u_i \in \mathfrak{lie}_n$ for $i = 1, ..., n$. Let $\mathrm{TAut}_n := \exp(\mathfrak{tder}_n)$ denote the group of *tangential automorphisms* – that is, basis conjugating automorphisms – of $\mathfrak{lie}_n$.

Let $F \in \mathrm{TAut}_2$, and assume that F is given by $F = (a_1, a_2)$, where $a_i = a_i(x, y)$, $F(x) = a_1^{-1} x a_1$, and $F(y) = a_2^{-1} y a_2$. We use cosimplicial notation in superscripts, for example:

- $F^{23} \in \mathrm{TAut}_3$ is given by (b_1, b_2, b_3), where $b_1 = 1$ (i.e., $F^{23}(x) = x$), $b_2 = a_1(y, z)$ and $b_3 = a_2(y, z)$.
- $F^{(12)3} \in \mathrm{TAut}_3$ is given by (b_1, b_2, b_3), where $b_1 = b_2 = a_1(x + y, z)$, and $b_3 = a_2(x + y, z)$.

The universal enveloping algebra of $\mathfrak{lie}_n$ is the free associative algebra A_n. The linear quotient $\mathrm{cyc}_n := A_n/[A_n, A_n]$ is the vector space of *cyclic words* in letters $x_1, ..., x_n$, and there is a natural trace map $\mathrm{tr} : A_n \to \mathrm{cyc}_n$. There is a *divergence 1-cocycle* $\div : \mathfrak{tder}_n \to \mathrm{cyc}_n$, given by $\div(u = (u_1, ..., u_n)) = \sum_{k=1}^n \mathrm{tr}(x_k(\partial_k u_k))$. Here ∂_k expands u_k as a sum of associative words, deletes those words whose last letter is not x_k, and deletes the last letter of words where the last letter is x_k. Thus, $\mathrm{tr}(x_k(\partial_k u_k))$ picks out words in u_k whose last letter is x_k and considers them as cyclic words.

The additive Jacobian cocycle $j : \mathrm{TAut}_n \to \mathrm{cyc}_n$ is given by:
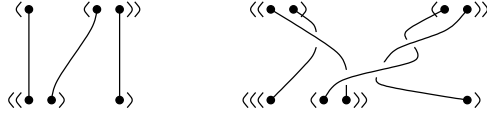
4

Figure 1. Two examples of parenthesized braids. Note that by convention the parenthetization can be read from the distance scales between the endpoints of the braid, and so we omit the parentheses in parts of this paper.

- the cocycle condition $j(gh) = j(g) + g \cdot j(h)$ (where the action of TAut_n on cyc_n is induced by the natural action of TAut_n on $\mathfrak{lie}_n$)
- the porperty $\frac{d}{ds} j(\exp(su))|_{s=0} = div(u)$ for all $u \in \mathfrak{tder}_n$.

We present an equivalent, modified version of the [AT, Section 5.3] formulation of the KV equations. The proof that this version is equivalent to the original follows from several Lemmas ~~of Alekseev–Enriquez–Torossian~~ ([AT, Theorem 7.5, Prop 9.3], [AET, Porp 7]). In Appendix A we give a short direct proof.

Definition 1.1. For $F \in \mathrm{TAut}_2$, denote by $\Phi_F \in \mathrm{TAut}_3$ the product $\Phi_F = (F^{(12)3})^{-1}(F^{12})^{-1}F^{23}F^{1(23)}$. The automorphism F is a *Kashiwara–Vergne solution* if it satisfies the two *Kashiwara–Vergne equations*:

$$F(x + y) = \log(e^x e^y) \tag{KV1}$$
$$j(\Phi_F) = 0 \tag{KV2}$$

1.2.2. *Topology.* We begin by describing a chain of maps from "parenthesized braids" to "(signed) knotted trivalent graphs" to "w-tangled foams":

$$\mathcal{K} := \{ uPaB \xrightarrow{\mathrm{cl}} sKTG \xrightarrow{a} \widetilde{wTF} \}.$$

Parenthesized braids are braids whose ends are ordered along two lines, the "bottom" and the "top", along with parenthetizations of the endpoints on the bottom and on the top. Two examples are shown in Figure 1. Parentehesized braids form a category whose objects are parenthetizations, morphisms are the parenthesized braids, and composition is given by stacking. In addition to stacking, there are several operations defined on parenthesized braids: strand addition, removal and doubling. A detailed introduction to parenthesized braids is in [BN1].

Trivalent graphs are oriented graphs with three edges meeting at each vertex and whose vertices are equipped with a cyclic orientation of the incident edges. A knotted trivalent graph (KTG) is a framed embedding of a trivalent graph into $\mathbb{R}^3$. KTGs are studied from a finite type invariant point of view in [BND1]. In this paper we use a version of KTGs that was introduced and studied in [WKO2, Section 4.6][2], namely trivalent tangles with one or two ends and with some extra combinatorial information: trivalent vertices are equipped with a marked "distinguished edge" and signs. We call this space *sKTG* (for signed KTGs), as in [WKO2]. An example is shown on the right. The space *sKTG* is also equipped with several operations: tangle insertion, sticking a 1-tangle onto an edge of another tangle,

---

[2]There is a 2024 Corrigendum [WKO2C] to [WKO2], specifically concerning Section 4. For readers' convenience, the Corrigendum's changes were incorporated into the arXiv version of [WKO2]. Hence, all specific section references to [WKO2] point to the arXiv v4 version, rather than the original published version.

5

disjoint union of 1-tangles, edge unzip, and edge orientation switch (see [WKO2, Section 4.6] for details).

The space $\widetilde{wTF}$ is a minor extension of the space wTF^o studied in [WKO2, Section 4.1 – 4.4], and will be introduced in detail in Section 2. Algebraically, it is described as a circuit algebra: similar to a planar algebra but with non-planar connections allowed, see [WKO2, Section 2.4] for a concise introduction, or [DHR1, Section 2] for a rigorous discussion. As a circuit algebra, $\widetilde{wTF}$ is generated by various kinds of crossings and "vertices", as well as "caps", modulo certain relations (Reidemeister moves), and equipped with a number of auxiliary operations beyond the circuit algebra compositions. This Reidemeister theory locally – and conjecturally globally – represents knotted tubes in 4-dimensional space with singular *foam vertices*, caps, and attached one-dimensional strings.

The map cl : $uPaB \to sKTG$ is the "closure map". Given a parenthesized braid, close up its top and bottom each by gluing a binary tree according to the parentetization; this produces a $sKTG$ with the convention that all strands are oriented upwards, bottom vertices are negative, and top vertices are positive. An example is shown below.

$$ \tag{1} $$
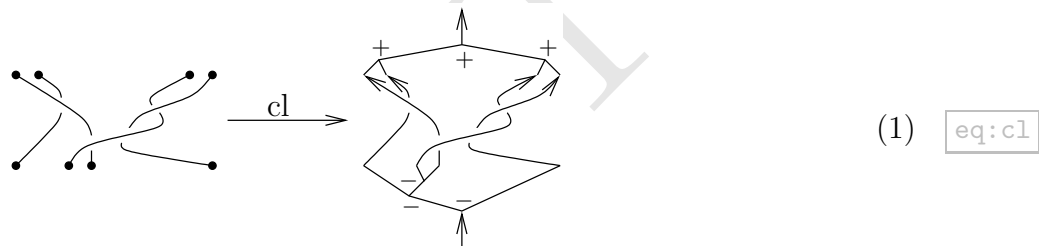
The map $a : sKTG \to \widetilde{wTF}$ arises combinatorially from the fact that all $sKTG$ diagrams can be interpreted as elements of $\widetilde{wTF}$, and $sKTG$ Reidemeister moves are also imposed in $\widetilde{wTF}$. Topologically, it is an extended version of Satoh's tubing map, described in Remark 3.1.1 of [WKO2].

1.2.3. *Algebra.* The chain of maps $\mathcal{K}$ is an example of a general "algebraic structure", as discussed in [WKO2, Section 2.1]. An algebraic structure consists of a collection of objects belonging to a number of "spaces" or "different kinds", and operations that may be unary, binary, multinary or nullary, between these spaces. In this case there are many spaces (or kinds of objects): for example, parenthesized braids with specified bottom and top parenthetizations form one space, so do knottings of a given trivalent graph (skeleton). There is a large collection of operations, consisting of all the internal operations of $uPaB$, $sKTG$ and $\widetilde{wTF}$, as well as the maps a and cl.

In Sections 2.1 to 2.3 of [WKO2] we discuss associated graded structures and expansions for general algebraic structures. For any algebraic structure (think braids, or tangles with tangle composition), one allows formal linear compositions of elements of the same *kind* (in this case, knotted objects with the same skeleton: braids with the same underlying permutation, or tangles with the same connectivity of endpoints and same number of circle components).

Associated graded structures are taken with respect to the filtration by powers of the *augmentation ideal*. For the spaces $uPaB$, $sKTG$ and $\widetilde{wTF}$, the associated graded spaces $\mathcal{A}^{hor}$, $\mathcal{A}^u$ and $\mathcal{A}^{sw}$ are the spaces of "horizontal chord diagrams on parenthesized strands", "chord diagrams on trivalent skeleta", and "arrow diagrams", as described in [BN1], [WKO2, Section 4.6], and Section 2 of this paper, respectively. Thus, the associated graded structure

6

of $\mathcal{K}$ is

$$\mathcal{A} := \{\mathcal{A}^{hor} \xrightarrow{\ \mathrm{cl}\ } \mathcal{A}^{u} \xrightarrow{\ \alpha\ } \mathcal{A}^{sw}\},$$

where cl and α are the maps induced by cl and a, respectively. More specifically, cl is the "closure of chord diagrams", and α is "replacing each chord with the sum of its two possible orientations", see [WKO2, Section 3.3].

An expansion [WKO2, Section 2.3] is a filtered map from an algebraic structure to its associated graded structure, whose associated graded map is the identity. In knot theory, expansions are also known as universal finite type invariants. A homomorphic expansion is an expansion which behaves well with respect to the operations of the algebraic structure, that is, it intertwines each operation with its induced counterpart on the associated graded structure. (For a more detailed introduction see [WKO2, Section 2.3].) Hence, a homomorphic expansion $Z : \mathcal{K} \to \mathcal{A}$ is a triple of homomorphic expansions Z^b, Z^u, and Z^w for $\mathcal{K}^b := uPaB$, $\mathcal{K}^u := sKTG$ and $\mathcal{K}^w := \widetilde{uTF}$, respectively, so that the following diagram commutes:

$$\mathcal{K}: \qquad \mathcal{K}^b \xrightarrow{\ \mathrm{cl}\ } \mathcal{K}^u \xrightarrow{\ a\ } \mathcal{K}^w \qquad\qquad (2)$$
$$\Big\downarrow{\scriptstyle Z} \qquad \Big\downarrow{\scriptstyle Z^b} \qquad \Big\downarrow{\scriptstyle Z^u} \qquad \Big\downarrow{\scriptstyle Z^w}$$
$$\mathcal{A}: \qquad \mathcal{A}^{hor} \xrightarrow{\ \mathrm{cl}\ } \mathcal{A}^u \xrightarrow{\ \alpha\ } \mathcal{A}^w$$

1.2.4. *The main result.* We recall [BN1] that a homomorphic expansion Z^b for parenthesized braids is determined by a *horizontal chord associator* or *Drinfel'd associator* $\Phi = Z^b(|\diagup|)$. A homomorphic expansion Z^u of *sKTG* is also determined[3] by a ~~Drinfel'd~~ associator (horizontal chords or not; see [WKO2, Section 4.6]), so the significance of the left commutative square is to force the associator corresponding to Z^u to be a horizontal chord associator. In turn, Z^w is determined by a solution F to the Kashiwara-Vergne problem (see [WKO2, Section 4.4 – 4.5]). The goal of this paper is to prove the following theorem, which, via the correspondence above, implies the Kashiwara-Vergne Theorem:

Theorem 1.2.   (1) *Assuming that $Z : \mathcal{K} \to \mathcal{A}$ exists, it is determined[4] by Z^u.*

(2) *Let $C = Z^w(\,\downarrow\,)$, then C is given by a power series with even part $C_0 = \alpha(\nu^{1/4})$, where ν is the Kontsevich integral of the unknot. There is a formula for $V = Z^w(\nearrow_\leftarrow))$ in terms of C and the Drinfel'd associator Φ associated to Z^u:*

$$V = C_1^{-1} C_2^{-1} \varphi \left(\Phi^{-1}(a_{2(13)}, -a_{2(13)} - a_{4(13)}) \cdot e^{a_{23}/2} \Phi(a_{23}, a_{43}) \right) C_{(12)}, \qquad (3)$$

where α denotes a single arrow[5]. This agrees[6] with the formula proven in [AET].

(3) *Every Z^b extends to a Z.*

Remark 1.3. The formula in part (2) of the Theorem, expresses $V = Z^w(\nearrow_\leftarrow))$ in terms of the Drinfel'd associator Φ, and $C = Z^w(\,\downarrow\,)$. One might wonder if there are separate formulas for both V and C in terms of Φ. In fact, in Corollary 3.13 we compute the "even part" of C explicitly, and show that it is fixed, in other words, does not depend on Φ. Part (1) of the

---

[3]With the exception of some minor normalization, see [WKO2], Lemma 4.14 and the paragraph after.

[4]In fact, almost entirely determined by Z^b, with the exception of some minor normalization of Z^u which is not determined by an associator.

[5]The notation is explained in detail in Section 3.2

[6]The two formulas are written in different languages, and checking that they agree takes effort. See Section 3.2 and Appendix A.

Theorem, proven in Section 3.1.2, shows that the complete value of C (even and odd part) is uniquely determined by Φ. In Theorem 3.6 we also prove that a suitable value exists for any choice Φ.

The key to the proof of the theorem is to show that the generator $\mathcal{J}_{\kappa}$ of $\widetilde{wTF}$ can be expressed in terms of the generator $|\diagup|$ of $uPaB$ and the operations of $\mathcal{K}$. Assuming that Z exists, this yields a formula for V in terms of Φ.

1.3. **Computations.** We note that this paper is "abstract", yet everything difficult in it occurs within graded spaces, and can be computed explicitly up to a certain degree. The highest degree to which computations can be completed depends on the specific object. In a follow-up paper [WKO4] many of these computations are carried out.

1.4. **Paper Structure.** In Section 2 we provide an overview of the space wTF^o of (oriented) w-foams and its extension with strings $\widetilde{wTF}$. We provide a brief review of definitions and crucial facts from [WKO2], and details of the extension. We prove that homomorphic expansions for wTF^o extend uniquely to homomorphic expansions for $\widetilde{wTF}$.

Section 3 makes up the bulk of the paper and is devoted to the proof of Theorem 1.2. In Section 3.1 we prove part (1). In Section 3.2 we deduce the formula for Kashiwara-Vergne solutions in terms of Drinfel'd associators, proving part (2). In Section 3.3 we prove statement (3), the hardest part of the proof.

Section **??** is a short section of closing remarks, and in Appendix A we give an explicit comparison and equivalence between our formula in Part (2) and the ALekseev–Enriquez–Torossian [AET] formula.

2. The spaces $\widetilde{wTF}$ and $\mathcal{A}^{sw}$ in more detail

The circuit algebra [WKO2, Section 2.4] of w-foams we use in this paper, $\widetilde{wTF}$, is an extension of the space wTF^o studied in [WKO2, Section 4.6]. As in [WKO2], $\widetilde{wTF}$ is given as a finite presentation in terms of generators and relations, with "auxiliary" operations in addition to the circuit algebra compositions. Our notation for such a presentation is:

$$CA\langle \text{ generators} \mid \text{relations} \mid \text{auxiliary operations} \rangle$$

Each generator and relation of $\widetilde{wTF}$ has a local topological interpretation, and so do the auxiliary operations, as follows. Recall from [WKO2] that wTF^o diagrams represent certain ribbon knotted tubes with foam vertices in $\mathbb{R}^4$, and there is a surjection δ, known as Satoh's tube map, from the circuit algebra wTF^o to such tubes. The space $\widetilde{wTF}$ extends wTF^o by adding one-dimensional strands to the picture. In themselves, one dimensional strands in $\mathbb{R}^4$ are never knotted, however, they can be knotted *with* the two-dimensional tubes. In figures two-dimensional tubes are denoted by thick lines and one dimensional strings by thin red lines. With this in mind, $\widetilde{wTF}$ is defined as:

$$\widetilde{wTF} = \text{CA}\Big\langle \underset{1}{\diagdown\!\!\!\diagup}, \underset{2}{\diagdown\!\!\!\diagup}, \underset{3}{\bullet\!\!|}, \underset{4}{\mathcal{J}_{\kappa}}, \underset{5}{\mathsf{Y}}, \underset{6}{\diagup\!\!\!\diagdown}, \underset{7}{\diagup\!\!\!\nearrow}, \underset{8}{\curlywedge}, \underset{9}{\longrightarrow} \Big| \begin{array}{c} \text{relations} \\ \text{as in} \\ \text{Section 2.2} \end{array} \Big| \begin{array}{c} \text{auxiliary} \\ \text{operations as} \\ \text{in Section 2.3} \end{array} \Big\rangle$$
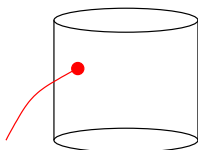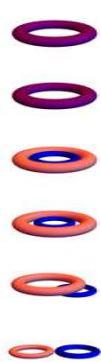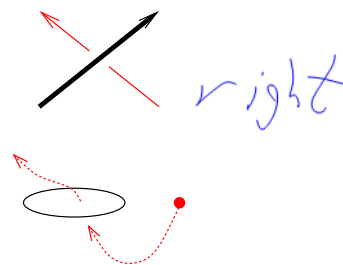
$$\text{generators}$$

Figure 2. A string-tube vertex.

2.1. **The generators of** $\widetilde{wTF}$**.** In this section we discuss the local topological meaning of each of the generators.

The first five generators are as described in [WKO2, Section 4.2.1], we briefly recall their descriptions here. Knotted (more precisely, braided) tubes in $\mathbb{R}^4$ can equivalently be thought of as movies of flying circles in $\mathbb{R}^3$. The two crossings stand for movies where two circles trade places by the circle of the under strand flying through the circle of the over strand. The dotted end represents a tube "capped off" at the bottom by a disk. Generators 4 and 5 stand for singular "foam vertices". The vertex 4 represents the movie shown on the left: the right circle approaches the left circle from below, flies inside it and merges with it. The vertex 5 represents a circle splitting and the inner circle subsequently flying out below and to the right. We note that as a circuit algebra, $\widetilde{wTF}$ has more vertex generators then shown above: the vertices come in all possible orientations of the strands, but we suppress the rest for brevity, and note that all other versions can be obtained from the ones shown using the "orientation switch" operations (to be discussed in Section 2.3).

The thin red strands denote one dimensional strings in $\mathbb{R}^4$, or "flying points in $\mathbb{R}^3$". The crossings between the two types of strands (generators 6 and 7) represent points flying through circles. For example, the picture on the left shows generator 6, where the point on the right approaches the circle on the left from below, flies through the circle and out to the left above it. Since a circle cannot fly through a point, there are no generators where a thick strand crosses under a thin red strand.

Generator 8 is a trivalent vertex of 1-dimensional strings in $\mathbb{R}^4$. Finally, the generator 9 is a *mixed vertex:* a one-dimensional string attached to the wall of a 2-dimensional tube, as shown in Figure 2. Mixed vertices are not rigid: there is no total orientation of edges included in the vertex data. (In other words, it doesn't matter which side of the thick black line the string is attached to.) These generators too exist in all possible strand orientation combinations; we are suppressing some of these to save space.

2.2. **The relations.** As a list, the relations for $\widetilde{wTF}$ are the same as the relations for wTF^o [WKO2, Section 4.6]: {R1^s, R2, R3, R4, OC, CP}. Recall that R1^s is the weak (framed) version of the Reidemeister 1 move; R2 and R3 are the usual second and third Reidemeister moves; R4 allowes moving a strand over or under a vertex. OC stands for *Overcorssings Commute*, CP for *Cap Pullout*: these two relations are shown in Figure 3, for a detailed explanation see [WKO2, Section 4.2.2].
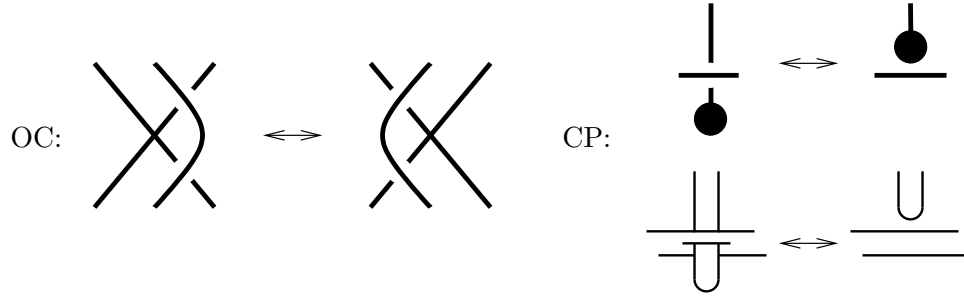
9

Figure 3. The OC and CP relations.

In $\widetilde{wTF}$ all relations should be interpreted in all possible combinations of strand types and orientations (tube or string), for example the under strand of the R2 relation can either be thick black or thin red, as shown below:

Similarly, any of the under strands of the R3, R4, and OC relations may be thin red.

As in wTF^o, the relations represent local isotopies of welded (ribbon knotted) tubes in $\mathbb{R}^4$ with singular vertices and attached strings. For example, Reidemeister 2 with a thin red bottom strand represents the movie isotopy between the movies where, on one hand, a point flies in through a circle and then immediately flies back out, and on the other hand, the constant movie. It is easy to verify that all relations indeed represent local isotopies, however, it is not clear whether the set of relations is complete. Conjecturally, $\widetilde{wTF}$ gives a Reidemeister theory for ribbon knotted tubes in $\mathbb{R}^4$ with caps, singular foam vertices and attached strings.

2.3. **The operations.** Like wTF^o, $\widetilde{wTF}$ is equipped with a set of auxiliary operations in addition to the circuit algebra structure.

The first of these is edge orientation switch (S_e), which reverses the direction of an edge (thick black or thin red).

The unzip operation u_e doubles the strand e using the blackboard framing, and then attaches the ends of the doubled strand to the connecting ones, as shown in Figure 4. We restrict unzip to edges that are the *stem* of each of the two vertices they connect, and whose two vertices have their inner and outer edges aligned, as shown (in other words, edges which connect two different generating vertices). Topologically, the blackboard framing of the diagram induces a framing of the corresponding tube in $\mathbb{R}^4$ via Satoh's tubing map, and unzip is the act of "pushing the tube off of itself slightly in the framing direction". Note that unzips preserve the ribbon property. For more details see [WKO2, Section 4.2.3]

A related operation, *disc unzip* unzips a capped strand, pushing the tube off in the direction of the framing (for diagrams, in the direction of the blackboard framing). An example is shown in Figure 4; see [WKO2, Section 4.2.3] for details.

The global *wenjugation* operation arises from the fact that if a w-foam is composed with wens (cut open Klein bottles) at every tangle end, then these wens all cancel [WKO2, Lemma
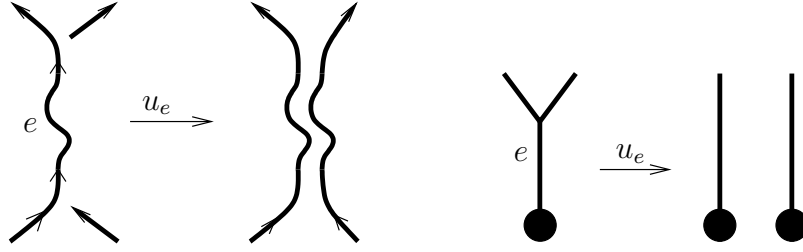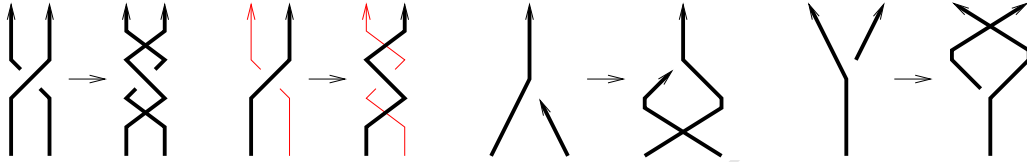
10

Figure 4. Unzip and disc unzip.

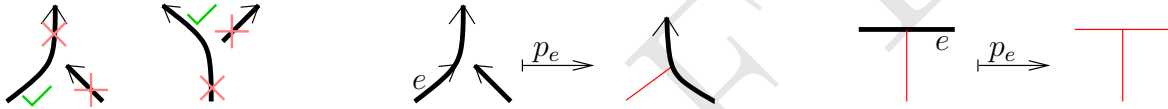**Figure 5.** The wenjugation operation.

Figure 6. Puncture operations: the picture on the left shows which edges can be punctured at each vertex. The middle and right pictures show the effect of puncture operations.

4.19]. The wenjugation of a w-foam F is denoted $\overline{F}$. Diagrammatically, wenjugation affects crossings and vertices as shown in Figure 5. Wenjugation composed with global orientation switch (switching the orientation of all edges) is called the *global adjoint* operation and denoted by $*$. That is, the adjoint of $F \in \widetilde{wTF}$ is F^*.

So far, all the operations had already existed in wTF^o. There is one new operation in $\widetilde{wTF}$ called "puncture" and denoted p_e, which turns the thick black edge e into a thin red one. In the local topological interpretation, this operation "punctures a tube", i.e., removes a small disk from it and retracts the rest to a one-dimensional core. Diagrammatically – and this is the rigorous definition – any crossings where e passes under another strand are not affected, while crossings in which e is the over strand turn into virtual crossings.

For technical reasons there is a restriction on which strands can be punctured, namely at each (fully thick black) vertex punctures are only allowed for one of the three meeting strands, as shown on the left of Figure 6. The right of the same figure shows that when puncturing one of the thick strands of a mixed vertex, the puncture "spreads": topologically, the mixed vertex represents a string attached to a tube, so when puncturing e, the entire tube retracts. Finally, a capped tube retracts to a point (disappears) when punctured.

In summary,

$$\widetilde{wTF} = \mathrm{CA} \left\langle \underset{1}{\text{⤬}}, \underset{2}{\text{⤬}}, \underset{3}{\text{•}}, \underset{4}{\text{⋋}}, \underset{5}{\text{⋎}}, \underset{6}{\text{⤬}}, \underset{7}{\text{⤬}}, \underset{8}{\text{⋏}}, \underset{9}{\text{⊢}} \;\middle|\; \begin{array}{c} \text{R1}^s,\, \text{R2},\, \text{R3},\\ \text{R4},\, \text{OC},\, \text{CP}\\ \text{relations} \end{array} \;\middle|\; \begin{array}{c} S_e,\, u_e,\, d_e,\, -,\, p_e\\ \text{auxiliary}\\ \text{operations} \end{array} \right\rangle$$

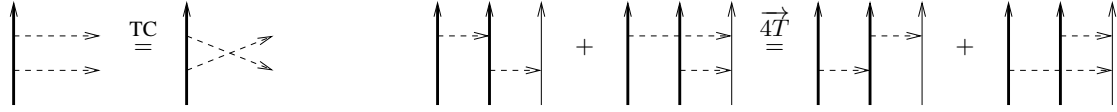$$\underbrace{}_{\text{generators}}$$

11

Figure 7. The TC and $\overrightarrow{4T}$ relations. Note that the 3rd strand in each term of the $\overrightarrow{4T}$ relation can be either thick black or thin red, the relation applies in either case.
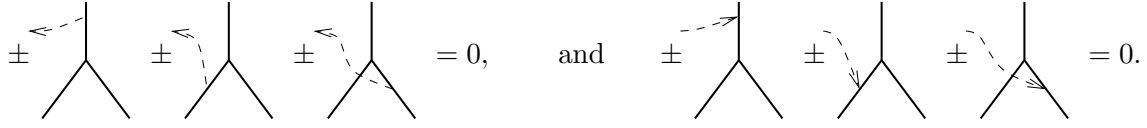
Figure 8. The VI relation: the vertices and strands could be of any type, but the same throughout the relation. The signs depend on the edge orientations: positive throughout it all edges are oriented the same way in relation to the vertex (all towards or all away from).
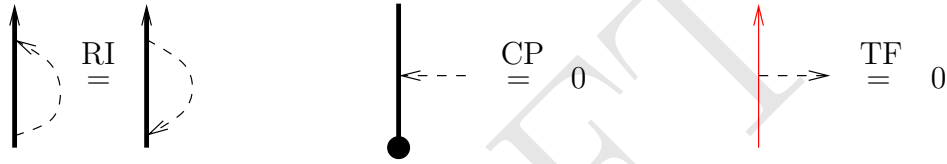
Figure 9. The RI and CP relations, and the TF relation (which is not really a relation).

2.4. The associated graded circuit algebra $\mathcal{A}^{sw}$.

As in [WKO2, Sections 4.6, 4.3], the space $\widetilde{wTF}$ is filtered by powers of its augmentation ideal. Its associated graded circuit algebra, denoted $\mathcal{A}^{sw}$, is a "space of arrow diagrams on foam skeletons with strings". As a circuit algebra, $\mathcal{A}^{sw}$ is presented as follows:

Generators 1 and 5 are the degree one generators, called arrows. The other generators are of degree zero, in other words, "skeleton features".

The relations are $\overrightarrow{4T}$ (the 4-Term relation), TC (Tails Commute), both shown in Figure 7; as well as the VI (Vertex Invariance, Figure 8); RI (Rotation Invariance), CP (the arrow Cap Pullout) and TF (Tails Forbidden on strings) - shown in Figure 9. Stating TF as a relation is a slight abuse of notation, as there are no generators with an arrow tail on a thin red strand, so saying that such an element vanishes is technically empty. However, without TF, the VI relation would have to be stated for all the sub-cases of 0, 1 or 3 thin red strands. All but the TF relation also appear in [WKO2, Section 4.6] as the relations of the associated graded circuit algebra of wTF^o.

Denote arrow diagrams on a given skeleton S, modulo relations, by $\mathcal{A}^{sw}(S)$. In particular, $\mathcal{A}^{sw}(\uparrow_n)$ denotes arrow diagrams on n (black) vertical strands, and $\mathcal{A}(\downarrow_n)$ denotes arrow diagrams on n capped strands.

Each operation on $\widetilde{wTF}$ induces a corresponding operation on $\mathcal{A}^{sw}$. The orientation switch S_e reverses the orientation of the skeleton strand e, and multiplies the arrow diagram by
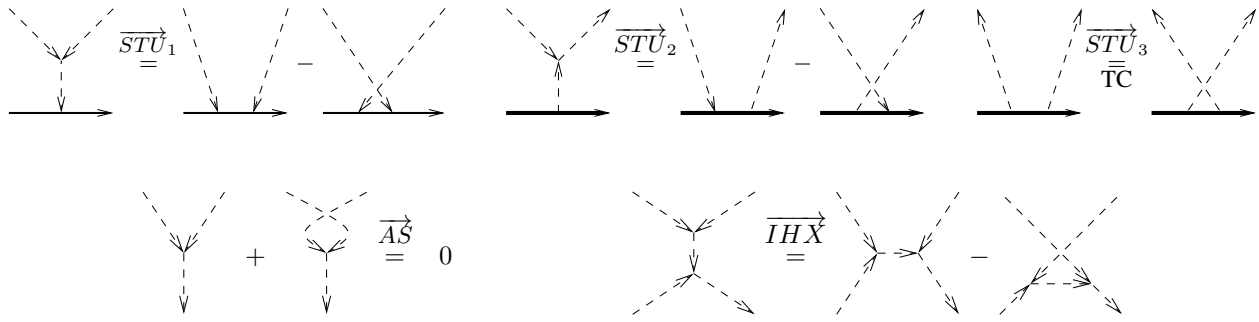
Figure 10. The $\overrightarrow{AS}$, $\overrightarrow{IHX}$ and the three $\overrightarrow{STU}$ rerations. Note that in $\overrightarrow{STU}_1$, the skeleton strand can be thin red or thick black, and that $\overrightarrow{STU}_3$ is the same as the TC relation.

$(-1)^{\#\{\text{arrow heads and tails on } e\}}$. The wenjugation operation multiplies the arrow diagram by $(-1)^{\#\{\text{arrow tails on } e\}}$. Given a skeleton S with a distinguished strand e, unzip (or disc unzip, if e is capped) is an operation $u_e : \mathcal{A}^{sw}(S) \to \mathcal{A}^{sw}(u_e(S))$ which maps each arrow ending on e to a sum of two arrows, one ending on each of the two new strands which replace e. Deleting a long strand e kills all arrow diagrams with any arrow ending on e. The operation induced by puncture, denoted p_e, turns the formerly thick black e into a thin red strand, and kills any arrow diagram with any arrow tails on e. All but the puncture operation are defined in the same way for wTF^o: for details see [WKO2, Section 4.2.2].

To summarise:

$$
\mathcal{A}^{sw} = \mathrm{CA} \left\langle \underbrace{\uparrow \text{-->} \uparrow}_{1}, \underbrace{\downarrow}_{2}, \underbrace{\nearrow}_{3}, \underbrace{\searrow}_{4}, \underbrace{\uparrow \text{-->} \uparrow}_{5}, \underbrace{\text{}}_{6}, \underbrace{\text{}}_{7} \;\middle|\; \begin{matrix} \overrightarrow{4T}, \text{TC, VI,} \\ \text{CP, RI, TF} \\ \text{relations} \end{matrix} \;\middle|\; \begin{matrix} S_e, u_e, d_e, -, p_e \\ \text{auxiliary} \\ \text{operations} \end{matrix} \right\rangle
$$

As in [WKO2, Definition 3.7], we define a "w-Jacobi diagram" (or just "arrow diagram") by also allowing trivalent chord vertices, each of which is equipped with a cyclic orientation, and modulo the $\overrightarrow{STU}$ relations of Figure 10. Denote the circuit algebra of formal linear combinations of these w-Jacobi diagrams by $\mathcal{A}^{swt}$. Then, as in [WKO2, Theorem 3.8], we have the following "bracket-rise" theorem:

Theorem 2.1. *The natural inclusion of diagrams induces a circuit algebra isomorphism $\mathcal{A}^{sw} \cong \mathcal{A}^{swt}$. Furthermore, the $\overrightarrow{AS}$ and $\overrightarrow{IHX}$ relations of Figure 10 hold in $\mathcal{A}^{swt}$.*

The proof is identical to the proof of [WKO2, Theorem 3.8]. In light of this isomorphism, we will drop the extra "t" from the notation and use $\mathcal{A}^{sw}$ to denote either of these spaces.

The space $\mathcal{A}^{sw}(\uparrow_n)$ forms a Hopf algebra with the stacking product and the standard co-product. (The coproduct is the sum over all possible ways of distributing the connected components of the arrow graph between two copies of the skeleton.) As in [WKO2], the primitive elements of $\mathcal{A}^{sw}(\uparrow_n)$ are connected diagrams, denoted $\mathcal{P}^{sw}(\uparrow_n)$, and $\mathcal{P}^{sw}(\uparrow_n) = \langle \text{trees} \rangle \oplus \langle \text{wheels} \rangle$ as a vector space. Examples of trees and wheels are shown in Figure 11; for details see [WKO2, Section 3.1]. Note that the RI relation can now be rephrased (via $\overrightarrow{STU}_2$) as the vanishing of the wheel with a single spoke, or one-wheel.

We recall the following crucial facts [WKO2, Proposition 3.19, Lemmas 4.6 and 4.7]:
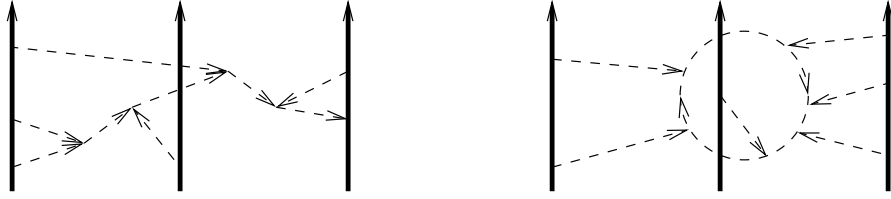
Figure 11. An example of a *tree*, left, and a *wheel*, right.

Fact 2.2. *As a Lie algebra, $\mathcal{P}^{sw}(\uparrow_n) \cong \langle wheels \rangle \rtimes \langle trees \rangle$. The vector space (abelian Lie algebra) spanned by wheels is canonically isomorphic to the space $(\mathrm{cyc}_n)_{\geq 1}$ of cyclic words[7] in n letters of degree at least 2, where degree is given by word length, and degree 1 is killed by the RI relation.*

Fact 2.3. $\mathcal{A}^{sw}(\downarrow)$, *the part of $\mathcal{A}^{sw}$ with skeleton a single capped strand, is isomorphic as a vector space to the completed polynomial algebra freely generated by wheels w_k with $k \geq 2$.*

Fact 2.4. $\mathcal{A}^{sw}(\nearrow_{\kappa}) \cong \mathcal{A}^{sw}(\uparrow_2)$, *where $\mathcal{A}^{sw}(\nearrow_{\kappa})$ stands for the space of arrow diagrams whose skeleton is a single vertex (the picture shows a positive vertex but the statement is true for all kinds of vertices with thick black strands), and $\mathcal{A}^{sw}(\uparrow_2)$ is the space of arrow diagrams on two (thick black) strands.*

The following Lemma – called the *Sorting Lemma* as we will see it "sorts" arrow tails above arrow heads – will play an important role. In particular the second isomorphism stated is the map φ appeacircle in Theorem 1.2, part (2). We will refer to the isomorphism φ in the Lemma as the *sorting isomorphism*.

Lemma 2.5 (Sorting Lemma)**.** *There is a linear isomorphism $\varphi : \mathcal{A}^{sw}\left(\begin{smallmatrix}\uparrow\\\bullet\end{smallmatrix}\right) \xrightarrow{\cong} \mathcal{A}^{sw}(\uparrow)$ between the vector spaces of arrow diagrams on the indicated skeleta. On the left, the thin red string is a tangle end. The black strand may continue past the arrow, and there may be additional skeleton components: the same on both sides. Applying the isomorphism φ twice, one obtains $\mathcal{A}^{sw}\left(\begin{smallmatrix}\nearrow\\\bullet\end{smallmatrix}\right) \stackrel{\varphi}{\cong} \mathcal{A}^{sw}(\uparrow_2)$.*

Proof. We construct inverse maps between the two spaces. There is a natural map $\mathcal{A}^{sw}(\uparrow) \xrightarrow{\psi} \mathcal{A}^{sw}\left(\begin{smallmatrix}\uparrow\\\bullet\end{smallmatrix}\right)$, shown in Figure 12: given an arrow diagram on a single thick black strand, place all arrow endings (denoted "x") on the strand above the tube/string vertex.

In the other direction, consider an arrow diagram on the capped/stringed vertex. One may assume that there are only arrow tails on the capped strand under the vertex: any arrow head may be commuted using $\overrightarrow{STU}$ relations towards the cap, where it is killed by the CP relation[8]. On the thin red strand there are only arrow heads. To construct φ, first "push" the arrow tails (denoted "t") from the capped strand up across the vertex using the VI relation. Since tails vanish on the thin red strand, they simply slide past the vertex. Once the capped side is cleared, continue by sliding the arrow heads "h" up from the thin red string to the strand above the vertex. Now the cap relation kills any arrow heads on

---

[7]Cyclic words are denoted $\mathfrak{tr}_n$ in [WKO2] and [AT] and $\mathfrak{T}_n$ in [AET].
[8]This argument also appears in [WKO2], for example as the basic idea for the proof of Fact 2.3.
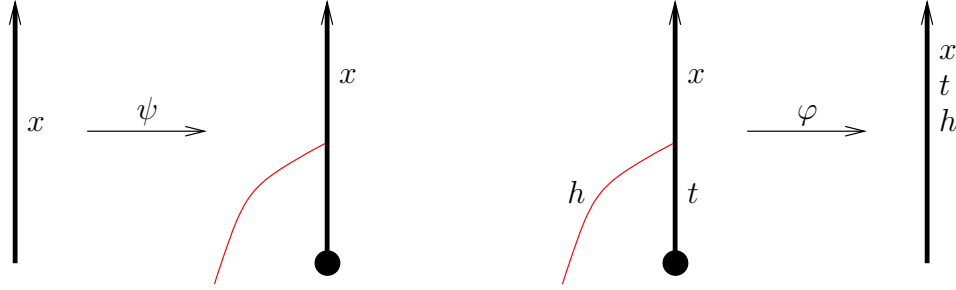
14

Figure 12. Inverse maps.

the capped strand, so once again they simply slide past the vertex. The result placed on a single thick black strand is shown in Figure 12.

It is clear that ψ is well-defined, we leave it to the reader to check that so is φ as a short exercise. Given that both maps are well-defined, it is clear that they are inverses of each other. $\qquad\square$

Observe that in the image of φ, all arrow tails are above arrow heads along the strand. Arrow diagrams of this form appear in the context of "over-then-under" tangles, which have applications in several contexts, including virtual braid classification [BDV].

2.5. **The homomorphic expansion.** As discussed in [WKO2, Section 2.3], an expansion for $\widetilde{wTF}$ is a map $Z^w : \widetilde{wTF} \to \mathcal{A}^{sw}$ with the property that the associated graded map $\operatorname{gr} Z^w : \mathcal{A}^{sw} \to \mathcal{A}^{sw}$ is the identity map $\operatorname{id}_{\mathcal{A}^{sw}}$. A homomorphic expansion is an expansion which also intertwines each operation of $\widetilde{wTF}$ with its arrow diagrammatic counterpart. In [WKO2, Theorems 4.9 and 4.11] we proved that the existence of solutions for the Kashiwara–Vergne equations implies that there exsists a homomorphic expansion for wTF^o. In fact that homomorphic expansions[9] for wTF^o are in one-to-one correspondence with solutions to the Kahiwara-Vergne problem.

The point of this paper is to provide a topological construction for such a homomorphic expansion (and hence for a solution of the Kashiwara–Vergne conjecture), and this is easier to do for the slightly more general space $\widetilde{wTF}$.

Let $\mathcal{A}^{osw} \subseteq \mathcal{A}^{sw}$ denote arrow diagrams on wTF^o skeleta, the associated graded space of wTF^o. One of the key results of [WKO2, Section 4.3] is the characterisation of homomorphic expansions of wTF^o. For any (group-like) homomorphic expansion $Z^{ow} : wTF^o \to \mathcal{A}^{osw}$, the value $Z^{ow}(\diagup\!\!\!\!\diagdown)$ is uniquely determined and equals $R = e^{a_{12}}$, where a_{12} denotes a single arrow from the over strand 1 to the under strand 2.

To state the full characterisation, we use co-simplicial notation in subscripts. For example, for $R = e^{a_{12}} = \in \mathcal{A}^{sw}(\uparrow_2)$, $R_{13} = e^{a_{13}}$ and $R_{23} = e^{a_{23}}$ in $\mathcal{A}^{sw}(\uparrow_3)$ are the diagrams where R is placed on strands 1 and 3, and 2 and 3, respectively. $R_{(12)3} \in \mathcal{A}^{sw}(\uparrow_3)$ is obtained by doubling the first strand of R and placing it on strands 1 and 2, and placing the second strand of R on strand 3, that is, $R_{(12)3} = e^{a_{13}+a_{23}}$. Similarly for $V \in \mathcal{A}(\uparrow_2)$, $V_{12} \in \mathcal{A}(\uparrow_3)$ denotes V placed on the first two starnds, et cetera.

Fact 2.6. *A filtered, group-like map $Z^{ow} : wTF^o \to \mathcal{A}^{osw}$ is a homomorphic expansion if and only if the Z^{ow}-values $V = Z^{ow}(\diagup\!\!\!\diagup)$ and $C = Z^{ow}(\,\downarrow\,)$ satisfy the following equations:*

---

[9]Subject to the minor technical condition that the value of the vertex doesn't contain isolated arrows.

(1) R4 Equation:
$$V_{12}R_{(12)3} = R_{23}R_{13}V_{12} \quad in \ \mathcal{A}^{sw}(\uparrow_3). \tag{R4}$$ eq:R4

(2) Unitarity Equation:
$$V \cdot A_1 A_2(V) = 1 \quad in \ \mathcal{A}^{sw}(\uparrow_2), \tag{U}$$ eq:U

where A_1 and A_2 denote the antipode operations.

(3) Cap Equation[10]:
$$C_{(12)}V_{12}^{-1} = C_1 C_2 \quad in \ \mathcal{A}^{sw}(\ \cdotp_2), \tag{C}$$ eq:C

where the subscripts mean strand placements as in the R4 Equation.

We begin by showing that finding a homomorphic expansion for $\widetilde{wTF}$ is no harder than finding one for wTF^o.

ndRestrict **Theorem 2.7.** *Homomorphic expansions for wTF^o are in one-to-one correspondence with homomorphic expansions for $\widetilde{wTF}$ via unique extension and restriction.*

Proof. Every element of wTF^o is also in $\widetilde{wTF}$, hence any Z^w restricts to a homomorphic expansion Z^{ow} of wTF^o. Every element of $\widetilde{wTF}$ is the result of puncturing – possibly on multiple strands – an element of wTF^o, and Z^w is required to commute with punctures. Hence any Z^{ow} uniquely extends to a Z^w. □

$$\begin{array}{ccc} wTF^o & \hookrightarrow & \widetilde{wTF} \\ \downarrow{\scriptstyle Z^{ow}} & & \downarrow{\scriptstyle Z^w} \\ \mathcal{A}^{osw} & \hookrightarrow & \mathcal{A}^{sw} \end{array}$$

In [WKO2, Section 4.4] we showed that short arrows – arrows whose head and tail is not separated by any other arrow endings – supported on either strand of V don't affect whether Z^w is a homomorphic expansion. That is, if Z^w is a homomorphic expansion and a is a linear combination of short arrows, then replacing V by $e^a V$ gives rise to another homomorphic expansion. Hence, in [WKO2] we typically assume there are no short arrows in V, this motivates the following definition:

Definition 2.8. A homomorphic expansion Z is *v-small* if there are no short arrows in the Z-value V of the positive vertex.

As it turns out, the value of the left-punctured vertex is trivial under any v-small homomorphic expansion. This fact will be useful later, so we prove it here.

lem:pV **Lemma 2.9.** *For any v-small homomorphic expansion Z^w, $Z^w\left(\ \right) = 1$, that is, the Z^w-value of a left punctured vertex is trivial.*

Proof. Recall from [WKO2, Proof of Theorem 4.9] that the Z^w-value V of the positive (not punctured) vertex can be written as $V = e^b e^t$, where b is a linear combination of wheels only and t (denoted uD in [WKO2]) is a linear combination of trees. puncturing the left strand of V kills all arrow diagrams with tails on the left strand. Diagrams that survive are wheels, and trees all of whose tails are on the right side strand. However, if all tails of a tree are supported on one strand, then the tree is a single arrow, due to TC and the anti-symmetry of the trivalent arrow vertices, thus the only surviving trees are simple arrows directed from right to left. Observe that all of these arrow diagrams commute with each other in $\mathcal{A}^{sw}(\uparrow_2)$.
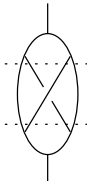
---

[10]For convenience we state the Cap Equation phrased for caps at the bottom of strands, hence the difference from the equivalent formulation in [WKO2].

16

Denote the value of the punctured vertex by $p_1 V = e^{p_1(b)} e^{p_1(t)}$. Recall that V must satisfy the Unitarity Equation of Fact 2.6, so $p_1 V \cdot A_1 A_2(p_1 V) = 1$. Since wheels have only tails, $A_1 A_2(p_1(b)) = p_1(b)$. Each arrow has one head, so $A_1 A_2(p_1(t)) = -p_1(t)$. Hence, using commutativity, $p_1 V \cdot A_1 A_2(p_1 V) = e^{2p_1(b)} = 1$, which implies that $p_1(b) = 0$. As for $p_1(t)$, one can show that there are no arrows pointing from the right to the left strand by a direct computation in degree 1. $\qquad\square$

3. Proof of Theorem 1.2

3.1. **Proof of Theorem 1.2 Part (1).** We prove Part 1 in two steps: first verifying the easier "tree level" case, which nonetheless contains the main idea, then in general.

3.1.1. *Tree level proof of Part (1).* Let $\mathcal{A}^{tree}$ denote the quotient of $\mathcal{A}^{sw}$ by all wheels, and let $\pi : \mathcal{A}^{sw} \to \mathcal{A}^{tree}$ denote the quotient map (cf [WKO2, Section 3.2]). Part (1) of the main theorem is the same as stating that Z^w is determined by Z^u. Z^w, in turn is determined by the values V and C of the positive vertex and the cap [WKO2, Sections 4.3 and 4.5], so one only needs to show that V and C are determined by Z^u. Proving this "on the tree level" means showing only that $\pi(V)$ and $\pi(C)$ are determined by Z^u. In particular, observe that since C is a linear combination of products of wheels (Fact 2.3), we have $\pi(C) = 1$, so we only need to show that $\pi(V)$ is determined by Z^u.

Let B^u denote the "buckle" *sKTG*, as shown on the right (ignore the dotted lines for now). All edges are oriented up, and by the drawing conventions of [WKO2, Section 4.6] all the vertices in the bottom half of the picture are negative and all the ones in the top half are positive. Let $B^w = a(B^u) \in \widetilde{uTF}$, and $\beta^u := Z^u(B^u)$. Note that β^u can be represented as a chord diagram on four strands[11]: use VI relations to move all chord endings to the "middle" of the skeleton, between the dotted lines on the picture. Hence, we write $\beta^u \in \mathcal{A}^u(\uparrow_4)$. Let $\beta^w = \alpha(\beta^u)$, and note that by the compatibility of Z^u and Z^w we have $\beta^w = Z^w(B^w)$. We will perform a series of operations on B^w and $\pi(\beta^w)$ to recover $\pi(V)$ from it.

$$B^u = \quad$$

First, connect (a circuit algebra operation in $\widetilde{uTF}$) a positive vertex to the bottom of B^w, as shown in Figure 13. Then unzip the edge marked by u, and puncture the edges marked e and e'. Then attach a cap (once again a circuit algebra operation) to the thick black end at the bottom. Finally, unzip the capped strand.
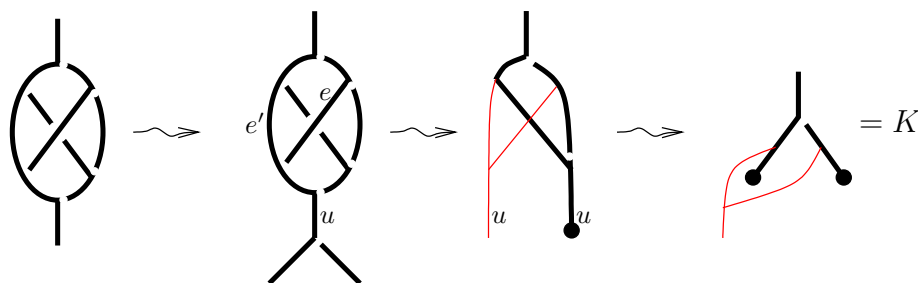

Figure 13. From the "buckle" β^w to the (modified) vertex.

---

[11]The value of β^u is computed explicitly to degree four in [WKO4].

Call the resulting w-foam K, as shown at the right in Figure 13. What is $Z^w(K)$? Due to the homomorphicity of Z, it is obtained from β^w by performing the same series of operations in the associated graded: a circuit algebra composition with V, unzip, punctures, circuit algebra composition with C, and disc unzip. Notice that the left strand of that attached vertex got punctured, and hence by Lemma 2.9 the attached value V cancels.[12] $Z^w(K)$ still depends on the value C. At the tree level, since $\pi(C) = 1$, $\pi(Z^w(K))$ can be computed from β^w by performing punctures and unzips. Since $\beta^w = \alpha(\beta^u)$, this means that $\pi(Z^w(K))$ is determined by Z^u.

On the other hand, note that the space of chord diagrams on the skeleton of K is the space $\mathcal{A}(\uparrow_2)$ by the Sorting Lemma (Lemma 2.5) and VI. Note also that K is a circuit algebra combination of a vertex, two left-punctured right-capped vertices and an all-red-strings vertex, and the Z^w-values of the latter three are trivial. So $\pi(Z^w(K)) = \pi(V) \in \mathcal{A}^{tree}(\uparrow_2)$. Hence, $\pi(V)$ is determined by Z^u as needed. □

3.1.2. *Complete proof of Theorem 1.2 Part (1).* In the previous subsection we showed that Z^u determines $\pi(V) \in \mathcal{A}^{tree}(\uparrow_2)$. The proof of Part (1) is completed by the following Lemma:

Lemma 3.1. *For any homomorphic expansion Z^w of $\widetilde{wTF}$ set $V = Z^w(\lambda_\cdot)$ and $C = Z^w(\cdot)$. Then $\pi(V) \in \mathcal{A}^{tree}(\uparrow_2)$ determines both V and C uniquely.*

Proof. We use a perturbative argument. By contradiction, assume this is not the case, in particular, first assume that there exist $V \neq V'$, both of which are vertex values of Z^u-compatible homomorphic expansions, such that $\pi(V) = \pi(V')$. Let v denote the lowest degree term of $V - V'$. Note that v is primitive and $v \in \ker \pi$, so v is a homogeneous linear combination of wheels. By the Unitarity Equation of Fact 2.6, we have $A_1A_2(v) = -v$. Recall that A_i reverses the direction of the strand i and multiplies each arrow diagram by (-1) to the number of heads on that strand. Since v has only tails, $A_1A_2(v) = v$, so $v = -v$, so $v = 0$, a contradiction. Therefore, $\pi(V)$ determines V uniquely.

Now we show that V determines C uniquely. Assume there are different values C and C' in $\mathcal{A}^{sw}(\cdot)$ so that (V, C) and (V, C') are both vertex-cap value pairs of Z^u-compatible homomorphic expansions. Let c denote the lowest degree term of $C - C'$, then c is a scalar multiple of a single wheel. The Cap Equation of Fact 2.6 implies $c_{(12)} = c_1 + c_2$ in $\mathcal{A}^{sw}(\cdot_2)$.

There is a well-defined linear map $\omega : \mathcal{A}^{sw}(\cdot_2) \to \mathbb{Q}[x, y]$ sending an arrow diagram – which has arrow tails only on each strand – to "x to the power of the number of tails on strand 1, times y to the power of the number of tails on strand 2". Assume $c = \alpha w_r$, where w_r denotes the r-wheel, and $\alpha \in \mathbb{Q}$. Then $0 = \omega(c_{(12)} - c_1 - c_2) = \alpha((x + y)^r - x^r - y^r)$, so either $r = 1$ or $\alpha = 0$. But $w_1 = 0$ in $\mathcal{A}^{sw}$ by the RI relation, hence $\alpha = 0$ and thus $c = 0$, a contradiction. □

3.2. **Proof of Theorem 1.2 Part (2).** In this section we compute V, the value of the vertex, from Φ, the Drinfel'd associator determining Z^b, using the construction of Part (1). In Appendix A we also show that this result translates to the [AET] formula for Kashiwara-Vergne solutions in terms of Drinfel'd associators.

In the computation of V from Φ, as well as later in the paper, we use two facts about Drinfel'd associators. We summarise these in the following Lemma:

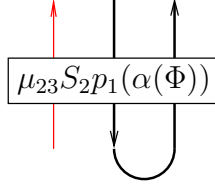[12]Any short arrows would also cancel when the right strand is capped.

Figure 14. A concatenated associator.

Lemma 3.2. *Let* $\Phi = \Phi(c_{12}, c_{23}) \in \mathcal{A}^u(\uparrow_3)$ *be a Drinfel'd associator, where* c_{ij} *denotes a chord between strands i and j. Let* $\alpha(\Phi) \in \mathcal{A}^w(\uparrow_3)$ *denote the image of* Φ *in arrow diagrams. Then, the following facts hold:*

(1) $\Phi(x, y) = \Phi(x, -x - z)$, *whenever* $(x + y + z)$ *is central.*
(2) $p_i p_j \alpha(\Phi) = 1$, *whenever* $i, j \in \{1, 2, 3\}$, $i \neq j$, *and* p_i *denotes puncture of the i-th strand.*
(3) $\mu_{23} \left(S_2 p_1(\alpha(\Phi)) \right) = 1$, *where* S_2 *stands for orientation switch of strand 2, and* μ_{23} *is concatenation (multiplication) of strands 2 and 3 – a circuit algebra operation – as shown in Figure 14.*

Proof. Property (1) follows from the fact that the logarithm of Φ is a Lie series in x and y with no constant term.

To show Property (2), recall that if $\Phi(x, y)$ is a Drinfel'd associator, then $\Phi(0, y) = \Phi(x, 0) = 1$. Therefore $p_1 p_2 \alpha(\Phi) = 1$, because $p_1 p_2 \alpha(c_{12}) = p_1 p_2(a_{12} + a_{21}) = 0$. Similar reasoning shows that $p_2 p_3 \alpha(\Phi) = 1$. Finally, $p_1 p_3 \alpha(\Phi(c_{12}, c_{23})) = \Phi(a_{21}, a_{23})$, and since $[a_{21}, a_{23}] = 0$ by the TC relation, $\Phi(a_{21}, a_{23}) = 1$.

For Property 3, note that $p_1(\alpha(\Phi)) = \Phi(a_{21}, -a_{21} - a_{31})$. Thus, strands 2 and 3 carry only arrow tails, and these commute by the TC relation, and $S_2 p_1(\alpha(\Phi)) = \Phi(-a_{21}, a_{21} - a_{31})$. Furthermore, tails on strand 3 can be pulled to strand 2 through the concatenation, which identifies a_{21} with a_{31}. Therefore, $\Phi(-a_{21}, a_{21} - a_{31}) = \Phi(-a_{21}, 0) = 1$. $\qquad\square$

To compute V and prove Part (2) of Theorem 1.2, consider once again the w-tangled foam K on the right of Figure 13.

On one hand, $Z^w(K)$ can be computed directly from the generators: $Z^w(K) = C_1 C_2 V_{12} \in \mathcal{A}^{sw}(\uparrow_2)$, since the values of the left-punctured vertices are trivial. Hence, if we know $Z^w(K)$, we know V.

On the other hand, we can compute $Z^w(K)$, using the compatibility with Z^u, as follows. Note that B^u is the closure – in the sense of (1) – of the parenthesised braid B^b shown in Figure 15, $B^w = a(B^u)$. Using the notation $\beta^u = Z^u(B^u)$, and $\beta^w = Z^w(B^w)$, and by the compatibility of Z^w with Z^u, we have

$$\beta^w = Z^w(B^w) = \alpha(Z^u(B^u)) = \alpha(\beta^u).$$

How does $Z^w(K)$ differ from β^w? To obtain K, a vertex and a cap were attached to B^w, two strands were punctured and the cap unzipped, as in Figure 13. The Z^w-value of the added vertex cancels when its left strand is punctured, however, the value of the cap remains and is unzipped. Thus, in loose notation, $Z^w(K) = u(C) \cdot p^2(\beta^w)$, where p^2 denotes the two punctures – we will compute this value explicitly in terms of associators shortly.
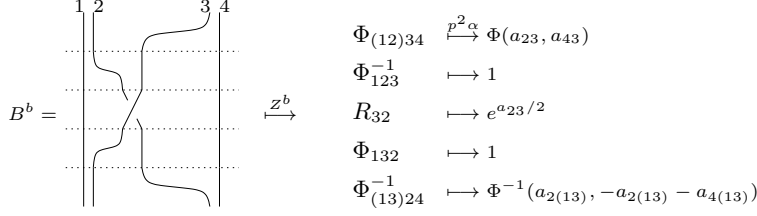
19

$$\Phi_{(12)34} \xmapsto{p^2\alpha} \Phi(a_{23}, a_{43})$$
$$\Phi_{123}^{-1} \longmapsto 1$$
$$B^b = \quad\xmapsto{Z^b}\quad R_{32} \longmapsto e^{a_{23}/2}$$
$$\Phi_{132} \longmapsto 1$$
$$\Phi_{(13)24}^{-1} \longmapsto \Phi^{-1}(a_{2(13)}, -a_{2(13)} - a_{4(13)})$$

Figure 15. Computing β^b. Strands are numbered at the top and multiplication is read from bottom to top; the rightmost column lists the images of the factors under $p_1p_3\alpha$.

To equate the two approaches, we need to express $u(C) \cdot p^2(\beta^w)$ as an element of $\mathcal{A}^{sw}(\uparrow_2)$, by applying the *sorting isomorphism* φ of Lemma 2.5. By doing so, we obtain

$$C_1 C_2 V_{12} = \varphi(u(C)p^2(\beta^w)). \tag{4}$$

Through a careful analysis of the right hand side, this will imply formula (3) stated in Theorem 1.2. In other words, we need to compute

$$\Upsilon := \varphi(u(C)p^2(\beta^w)).$$

To achieve this, we use that $\beta^w = \alpha(\beta^u)$, and compute β^u in terms of the Drinfel'd associator Φ associated to Z^u. By the compatibility of Z^u and Z^b, it is enough to compute $\beta^b := Z^b(B^b)$. The result can be read from the picture in Figure 15:

$$\beta^b = \Phi_{(13)24}^{-1} \Phi_{132} R_{32} \Phi_{123}^{-1} \Phi_{(12)34}.$$

Recall that the cosimplicial notation used in the subscripts show which strands the diagrams are placed on, for example, $\Phi_{(13)24}^{-1} = \Phi^{-1}(c_{12} + c_{32}, c_{24})$. Also recall that $R = e^{c/2}$, so $R_{32} = e^{c_{23}/2}$.

As β^u is the tree closure of β^b, it is given by the same formula interpreted as an element of $\mathcal{A}^u(\uparrow_4)$. One then applies α to obtain $\beta^w = \alpha(\beta^u)$. After the vertex and cap attachment, of Figure 13, strands 1 and 3 are punctured and strands 2 and 4 are capped, and in this strand numbering, $u(C) = C_{24}$ Therefore, we have

$$\Upsilon = \varphi\left(C_{24} \cdot p_1 p_3 \alpha (\Phi_{(13)24}^{-1} \Phi_{132} R_{32} \Phi_{123}^{-1} \Phi_{(12)34})\right).$$

Next, we analyse how the puctures and α act on factors of β^b. First observe that $p_3\alpha(R_{32}) = e^{a_{23}/2}$, where a_{ij} is a single arrow pointing from strand i to strand j.

Observe that $p_1 p_3 \alpha(\Phi_{123}^{-1}) = p_1 p_3 \alpha(\Phi_{123}^{-1}) = 1$ by Fact (2) of Lemma 3.2.

Since strands 1 and 3 are both punctured, no arrows can be supported between these two strands, hence $p_1 p_3 \alpha(\Phi_{(12)34}) = \Phi(a_{23}, a_{43})$.

By Properrty (1) of Lemma 3.2, $\Phi_{(13)24}^{-1} = \Phi^{-1}(c_{(13)2}, c_{24}) = \Phi^{-1}(c_{(13)2}, -c_{(13)2} - c_{(13)4})$, so $p_1 p_3 \alpha \Phi_{(13)24}^{-1} = \Phi^{-1}(a_{2(13)}, -a_{2(13)} - a_{4(13)})$. To summarise,

$$\Upsilon = \varphi\left(C_{24} \cdot \Phi^{-1}(a_{2(13)}, -a_{2(13)} - a_{4(13)}) \cdot e^{a_{23}/2} \cdot \Phi(a_{23}, a_{43})\right).$$

Note that the expression $\Phi^{-1}(a_{2(13)}, -a_{2(13)} - a_{4(13)}) \cdot e^{a_{23}/2} \cdot \Phi(a_{23}, a_{43})$ has only arrow tails on strands 2 and 4, and therefore commutes with C_{24} by the TC relation. Hence, by the
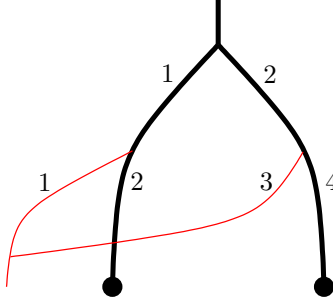
20

Figure 16. Strand numbering convention for K and V: arrow endings from strand 1 and 2 of K are "pushed" to strand 1 of V when applying φ, and arrow endings from strands 3 and 4 are pushed to strand 2.

definition of φ,

$$\Upsilon = \varphi\left(\Phi^{-1}(a_{2(13)}, -a_{2(13)} - a_{4(13)}) \cdot e^{a_{23}/2} \cdot \Phi(a_{23}, a_{43}) \cdot C_{24}\right)$$
$$= \varphi\left(\Phi^{-1}(a_{2(13)}, -a_{2(13)} - a_{4(13)}) \cdot e^{a_{23}/2} \cdot \Phi(a_{23}, a_{43})\right) \cdot \varphi(C_{24}).$$

Furthermore, by the strand numbering convention shown in Figure 16, we have $\varphi(C_{24}) = C_{12}$. Therefore,

$$V_{12} = C_1^{-1} C_2^{-1} \Upsilon = C_1^{-1} C_2^{-1} \varphi\left(\Phi^{-1}(a_{2(13)}, -a_{2(13)} - a_{4(13)}) \cdot e^{a_{23}/2} \cdot \Phi(a_{23}, a_{43})\right) C_{12},$$

as stated in part (2) of Theorem 1.2. □

In [WKO4] V is computed to degree 4 using the techniques of this section. Matching this result to the Alekseev–Enriquez–Torossian formula of [AET, Theorem 4.] is technical, and not used anywhere else in the paper, hence we defer this to Appendix A.

3.3. **Proof of Theorem 1.2 part (3): the double tree construction.** Given a homomorphic expansion Z^u of $sKTG$, in Section 3.1.2 we showed that if there is to exist a homomorphic expansion Z^w of $\widetilde{wTF}$ compatible with Z^u, then $V = Z^w(\lambda)$ and $C = Z^w(\downarrow)$, and hence Z^w itself, are uniquely determined by Z^u. In Section 3.2 we proved the formula (3), which in particular gives an explicit expression for the tree level value of V in terms of the Drinfel'd associator associated to Z^u. From here on we denote this value V_β^{tree} as it is calculated from the Z^u-value of the "buckle" graph:

$$V_\beta^{tree} = \varphi\left(\Phi^{-1}(a_{2(13)}, -a_{2(13)} - a_{4(13)}) e^{a_{23}/2} \Phi(a_{23}, a_{43})\right) \tag{5}$$

It remains to show that there exists an appropriate cap value $C = Z^w(\downarrow)$ such that C along with the value of the vertex as given in formula (3)

$$Z^w(\lambda) =: V_\beta = C_1^{-1} C_2^{-1} V_\beta^{tree} C_{(12)} \tag{6}$$

determine a homomorphic expansion of $\widetilde{wTF}$, which is furthermore compatible with Z^u. In particular, in order to show that the a pair (V_β, C) defines a homomorphic expansion, one needs to show that the values V_β and C satisfy the equations (R4), (U) and (C) of Fact 2.6. We do this in order of difficulty: first the easiest Cap Equation (C), then Unitarity (U) (assuming (R4) and compatibility), then Reidemeister 4 (R4) (hard). Finally, we prove compatibility, which is easier again, given the machinery developed for (R4).

Proposition 3.3. *For any choice of $C \in \mathcal{A}^{sw}(\downarrow)$, the values V_β and C verify (C).*

21

Proof. Substituting V_β and C into the Cap equation (C), we need to show that

$$u(C)(u(C))^{-1}(\varphi(p_1 p_3 \beta^w))^{-1}C_1 C_2 = C_1 C_2,$$

in $\mathcal{A}^{sw}(\,\downarrow_2)$. We cancel $u(C)(u(C))^{-1}$ on the left, and multiply on the right by $C_1^{-1}C_2^{-1}$ (this is valid as $\mathcal{A}(\,\downarrow_2)$ is a right $\mathcal{A}(\uparrow_2)$-module by stacking). Then we only need to show that $(\varphi(p_1 p_3 \beta^w))^{-1} = 1$ in $\mathcal{A}(\,\bullet_2)$. We can multiply on the right by $\varphi(p_1 p_3 \beta^w)$, hence it's enough to see that $1 = \varphi(p_1 p_3 \beta^w)$. This, in turn, is clear by the CP relation since all heads are below all tails in the image of φ. $\qquad\square$

To address the unitarity equation, we need to set up some notation prove a few basic Lemmas about arrow diagrams.

Definition 3.4. For an arrow diagram $D \in \mathcal{A}^{sw}(\uparrow_n)$ let D^*, the *adjoint* of D, be the arrow diagram $A_1 A_2 ... A_n(D)$, where A_i denotes the *adjoint* operation applied to strand i. For a group-like diagram[13] $D = e^d$, where $d \in \mathcal{P}^{sw}(\uparrow_n)$, denote by $\|D\|$ the diagram DD^*, and call it the "*norm*[14]" of D.

Lemma 3.5. *The adjoint operation and norm satisfy the following basic properties:*

(1) $(D_1 D_2)^* = D_2^* D_1^*$.

(2) *If $d \in \mathcal{P}^{sw}(\uparrow_n)$ is a primitive arrow diagram, then $(e^d)^* = e^{d^*}$.*

(3) *If $d \in \mathcal{P}^{sw}(\uparrow_n)$ is a wheel, then $d^* = d$, and $\|e^d\| = e^{2d}$.*

(4) *If $d \in \mathcal{P}^{sw}(\uparrow_n)$ is a tree, then $\|e^d\| \in \exp(\langle wheels \rangle)$.*

(5) *If $d_1, d_2 \in \mathcal{P}^{sw}(\uparrow_n)$, then $\|e^{d_1} e^{d_2}\| = \|e^{d_1}\|\|e^{d_2}\|^{e^{d_1^*}} = \|e^{d_1}\|\|e^{d_2}\|^{e^{-d_1}}$, where the exponent denotes conjugation.*

(6) *If $d \in \mathcal{P}^{hor}(\uparrow_n)$ is a primitive horizontal chord diagram, then $\|e^{\alpha(d)}\| = 1$.*

Proof. Properties (1), (2), and (3) are immediate from the definitions. Property (4) follows from the fact that for a tree arrow diagram d, the sum $(d + d^*)$ is a linear combination of wheels by repeated applications of $\overline{STU}$ relations.

We verify property (5) directly:

$$\|e^{d_1} e^{d_2}\| = e^{d_1} e^{d_2} e^{d_2^*} e^{d_1^*} = e^{d_1} e^{d_1^*} e^{-d_1^*} e^{d_2} e^{d_2^*} e^{d_1^*} = \|e^{d_1}\|\|e^{d_2}\|^{e^{d_1^*}}.$$

To show the second equality, note that by definition $e^{d_1^*} = e^{-d_1}\|e^{d_1}\|$. By Property (4), $\|e^{d_2}\| \in \exp(\langle wheels \rangle)$, so $\|e^{d_2}\|^{e^{-d_1}} \in \exp(\langle wheels \rangle)$. Since $\|e^{d_1}\| \in\in \exp(\langle wheels \rangle)$, it acts trivially on $\|e^{d_2}\|^{e^{-d_1}}$.

To prove property (6) observe that for a single chord $t_{ij} \in \mathcal{A}^{hor}$, $\alpha(t_{ij}) = a_{ij} + a_{ji}$, that is, the sum of arrows from strand i to strand j and vice versa. Therefore, $(\alpha(t_{ij}))^* = -\alpha(t_{ij})$. Furthermore, if in $\mathcal{P}^{sw}(\uparrow_n)$, x and y are two primitive arrow diagrams such that $x^* = -x$ and $y^* = -y$, then by direct computation we also have $([x,y])^* = -[x,y]$. Since the set $\{(t_{ij})\}_{1 \leq i < j \leq n}$ generate $\mathcal{P}^{hor}(\uparrow_n)$ as a Lie algebra, this implies that $(\alpha(d))^* = -\alpha(d)$ for any $d \in \mathcal{P}^{hor}(\uparrow_n)$. Thus, by direct computation

$$\|e^{\alpha(d)}\| = e^{\alpha(d)} e^{(\alpha(d))^*} = e^{\alpha(d)} e^{-\alpha(d)} = 1.$$

---

[13]While the definition of "norm" makes sense for all arrow diagrams, it is most useful, and only used, in the context of group-like diagrams.

[14]We use the word "norm" only because it is notationally intuitive; we do not claim that $\|D\|$ satisfies the properties of a norm. The reader might object that it should be called "norm squared"; in our opinion this would clutter up the notation too much.

$\square$

The following theorem states that any *tree-level* homomorphic expansion of $\widetilde{wTF}$ that is compatible to Z^u lifts to a genuine homomorphic expansion of $\widetilde{wTF}$.

Theorem 3.6. *Suppose that $Z^{tree} : \widetilde{wTF} \to \mathcal{A}^{tree}$ is a filtered map with $Z^{tree}(\mathcal{J}_{\mathfrak{c}}) := V^{tree}$, such that V^{tree} satisfies the (R4) equation, and for any $K \in sKTG$, $Z^{tree}(a(K)) = \pi\alpha Z^u(K)$. Then there exists a group-like $C \in \mathcal{A}^{sw}(\,\downarrow\,)$ which, along with $V := C_1^{-1}C_2^{-1}V^{tree}C_{12}$, defines a homomorphic expansion $Z^w : \widetilde{wTF} \to \mathcal{A}^{sw}$.*

Proof. Indeed, the values (V, C) uniquely determine Z. To show that Z is a homomorphic expansion, we need to prove that (V, C) satisfy the (R4), (C) and (U) equations. The (R4) equation only depends on V^{tree}. Since $\pi(V) = \pi(C_1^{-1}C_2^{-1}V^{tree}C_{12}) = V^{tree}$, therefore V satisfies (R4) by assumption. The fact that (V, C) satisfy the Cap (C) equation follows from Proposition 3.3.

For the remainder of this proof we denote $V^{tree} =: T$. The main difficulty is to show that (V, C) satisfy the Unitarity (U) equation, which can be re-stated as $\|V\| = 1$. Substituting $V = C_1^{-1}C_2^{-1}V^{tree}C_{12}$, the (U) equation becomes $C_1^{-1}C_2^{-1}TC_{12}^2 T^*C_2^{-1}C_1^{-1} = 1$, and by rearranging, this simplifies to

$$\|T\| = \left(\left((C_{12})^{T^{-1}} \right)^{-1} C_1 C_2 \right)^2, \tag{7}$$

where T^{-1} in the exponent denotes conjugation. We need to prove that there exists a value $C = e^c$, which satisfies this equation. Note that $\|T\|$ is an exponential of wheels in $\mathcal{A}^{sw}(\uparrow_2)$, so this makes semantic sense. By Fact 2.2, $\|T_{12}\|$ is identified with an element of $\exp(\mathrm{cyc}\langle x, y\rangle)$ and thus represented by an exponential in cyclic words in two variables. Let $f(x, y) \in \mathrm{cyc}\langle x, y\rangle$ denote the logarithm of $\|T\|$. In turn, $c \in \mathrm{cyc}\langle x\rangle \cong \mathbb{Q}[[x]]$, thus we write $c = c(x)$.

We claim that

$$(C_{12})^{T^{-1}} = (\exp(c(x + y)))^{T^{-1}} = T\exp(c(x + y))T^{-1} = \exp(c(\log(e^x e^y))).$$

The last equality follows from the fact that T satisfies the (R4) equation; this is explained in detail in [WKO2], Section 4.4, in particular in and around Fig. 19.

With this reduction in place (7) reduces to

$$e^{f(x,y)} = \left(e^{c(\log(e^x e^y))} e^{c(x)} e^{c(y)} \right)^2,$$

and since all exponents (wheels) commute, this is equivalent to

$$f(x, y) = 2\big(c(x) + c(y) + c(\log(e^x e^y))\big). \tag{8}$$
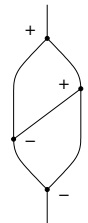
which we need to solve for $c \in \mathbb{Q}[[x]]$.

To do so, we use that $Z^{tree}(a(K)) = \pi\alpha Z^u(K)$, specifically for the associator graph $K = \phi$ shown on the right. Recall that $Z^u(\phi)$ is a Drinfel'd associator Φ. On the other hand, $\alpha(\phi)$ is a circuit algebra product of four vertices, therefore

$$\alpha(\Phi) = Z^{tree}(a(\phi)) = T_{12,3}^{-1}T_{12}^{-1}T_{23}T_{1,23}.$$

Rearranging, we obtain

$$T_{12}T_{12,3}\alpha(\Phi) = T_{23}T_{1,23}.$$

23

Applying the "norm" to both sides, keeping in mind that $\|\alpha(\phi)\| = 1$ by Lemma 3.5 property (6), and using the exponent notation for the adjoint action on a norm, we get

$$\|T_{12}\|\|T_{12,3}\|^{T_{12}^{-1}} = \|T_{23}\|\|T_{1,23}\|^{T_{23}^{-1}}. \tag{9}$$

Recall that $\|T_{12,3}\| = \exp(f(x+y,z))$, $\|T_{23}\| = \exp(f(y,z))$, $\|T_{1,23}\| = \exp(f(x,y+z))$.

As before, we have

$$\|T_{12,3}\|^{T_{12}^{-1}} = (\exp(f(x+y,z)))^{T_{12}^{-1}} = T_{12}\exp(f(x+y,z))T_{12}^{-1} = \exp(f(\log(e^x e^y),z)),$$

since T satisfies the (R4) equation. Similarly,

$$\|T_{1,23}\|^{T_{23}^{-1}} = (\exp(f(x,y+z)))^{T_{23}^{-1}} = \exp(f(x,\log(e^y e^z))).$$

Thus, Equation (9) reduces to

$$e^{f(x,y)}e^{f(\log(e^x e^y),z)} = e^{e^{f(y,z)}}e^{f(x,\log(e^y e^z))},$$

and since all the exponentials (wheels) commute, this is equivalent to

$$f(x,y) = f(y,z) + f(x,\log(e^y e^z)) - f(\log(e^x e^y),z) \tag{10}$$

The fact that there exists a solution $c(x)$ to Equation 8 follows from this equation via a short cohomology calculation as in [AET, Proposition 27], and [AT, Appendix A, Proof of Theorem 2.8]. □

In order to use Theorem 3.6, it is necessary to show that the value V^{tree} constructed in Section 3.1.1 satisfies the (R4) equation; unfortunately this is hard. The equation (R4) is an equality between different circuit algebra – in fact, planar algebra – compositions of crossings. Hence, the proof would be much easier if Z^u were to be a circuit algebra – or planar algebra – map. This unfortunately makes no sense, as *sKTG* is not a circuit or planar algebra but a different, more complicated algebraic structure.

The reader might ask, why work with a space as inconvenient as *sKTG* instead of, say, a planar algebra of trivalent tangles? The answer is that the existence of a homomorphic expansion is a highly non-trivial property, and in particular ordinary trivalent tangles do not have one. Even without trivalent vertices, ordinary tangles, or u-tangles, do not have have a homomorphic expansion as a planar algebra[15]. *Parenthesized tangles* (a.k.a. *q-tangles*) [LM, BN2] do have homomorphic expansions, yet in fact these are almost equivalent to *sKTG* [T, BND1, Da].

Nonetheless, we can harness the power of planar algebras in a less direct way to prove the R4 equation, by building a new definition for Z^w. Since we will be working with two constructions (eventually proving that they lead to the same expansion), it will be necessary to distinguish them, at least temporarily.

- From here on we denote the value V^{tree} arising from the "buckle" construction of Section 3.1.1 by V_β^{tree}. Assuming the conditions of Theorem 3.6 hold, there is a unique homomorphic expansion Z_β^w for which $\pi(Z^w(\lambda_\kappa)) = V_\beta^{tree}$.

_____

[15]We only mention that the planar algebra of u-tangles does not have a homomorphic expansion Z^t so as to explain why we are not using one. This said, the non-existance of Z^t is easy to prove: by an explicit calculation in degree 2 one shows that there is no linear combination of chord diagrams that can serve as $Z^t(\chi)$, satisfying the R3 relation.
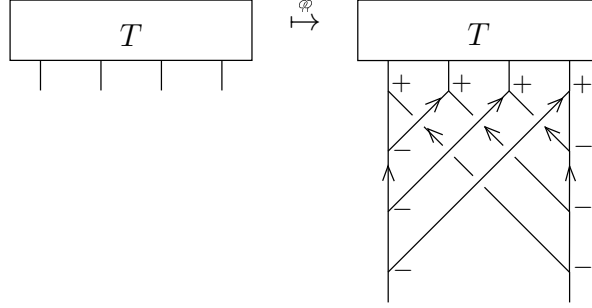
24

Figure 17. The *double tree map*: connect the ends of T by two binary trees (hence "double tree"), as shown. Note that the tree on the left always crosses over the tree on the right, and all edges of both trees are oriented towards T.

- In a new construction, we map classical trivalent tangles into *sKTG* via a "*double tree*" map, and use this to define a partial expansion Z_ξ^w for the *a*-images of classical trivalent tangles. This in particular defines a new vertex value $Z_\xi^w(\lambda_\kappa) = V_\xi$.
- After some technical lemmas, we show that Z_ξ^w satisfies the compatibilty $Z^w(a(K)) = \alpha Z^u(K)$ for all $K \in sKTG$: see Proposition 3.14.
- We show that restriction of Z_ξ^w to $a(uTT)$ is a planar algebra map (see Theorem 3.17), and thus Z_ξ^w satisfies the (R4) equation.
- We show that the two constructions yield the same vertex value on the tree level: $\pi(V_\xi) = V_\beta^{tree}$. This is done in Lemma 3.19. Thus, by Lemma 3.1, if the two constructions produce homomorphic expansions, those expansions are the same.
- Putting this together, V_β^{tree} satisfies (R4) and the compatibility condition of Theorem 3.6, and thus exists a unique homomorphic expansion $Z^w = Z_\xi^w = Z_\beta^w$, compatible with Z^u. We prove this in detail in Theorem 3.22 below.

3.3.1. *The new construction: Z_ξ^w.* We start by defining (classical, or *usual*) trivalent tangles, denoted *uTT*:

$$uTT := \mathrm{PA} \left\langle \ \nwarrow\!\!\!\!\nearrow, \ \nwarrow\!\!\!\!\nearrow, \ \lambda^+, \ \lambda^- \ \middle| \ \mathrm{R1}^s, \ \mathrm{R2}, \ \mathrm{R3}, \ \mathrm{R4} \ \middle| \ S_e, \ u_e \ \right\rangle$$

Here PA stands for *planar algebra*: an algebra over the operad of planar tangles, that is, an algebraic structure similar to a circuit algebra, except with *planar* wicircle diagrams. (See [DHR1, Section 3.1] for a detailed definition. This is a slightly more simple-minded notion than the original use of the term in [J], in particular we do not use checkerboard shadings.)

The elements of *uTT* are usual – that is, classical – trivalent tangles with ordered ends (the ordering is assumed to be counterclockwise from bottom left, unless otherwise stated), and signed vertices with a total ordering of edges at each vertex. There are no "virtual crossings" in planar algebras. The relations are the usual Reidemeister relations which make sense in this context (R1^s, R2, R3 and R4). The planar algebra *uTT* is equipped with auxiliary orientation switch and edge unzip operations. Edge unzips are defined for edges that connect a positive and a negative vertex in as shown in the figure on the right. The planar algebra *uTT* does not have a homomorphic expansion.
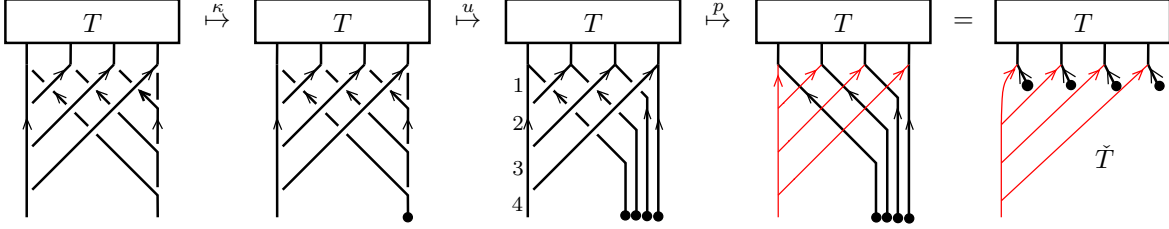
25
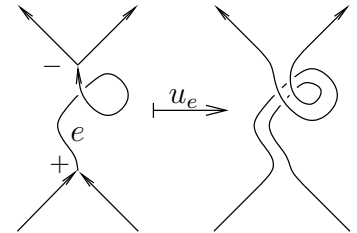
Figure 18. The cap attachment, unzips and punctures. While these operations are applied in $\mathcal{A}^{sw}$ – there are arrows on these skeleta – for simplicity the figure only shows the effect on the skeleton.

We define a *double tree* map $\mathscr{P} : u\!TT \to sKTG$, as in Figure 17. The map $\mathscr{P}$ depends on two choices of binary trees: in Figure 17 we chose a particular example. It is important that, regardless of the choice of trees, the "left side" tree crosses over the "right side" tree. We will demonstrate that in fact the choice of trees becomes irrelevant after some post-compositions, see Lemma 3.7.

Working towards a construction of Z_ξ^w, we post-compose $\mathscr{P}$ with the following sequence of maps, which are explained in the paragraph below:

$$T \in u\!TT \xrightarrow{\;\mathscr{P}\;} sKTG \xrightarrow{\;Z^u\;} \mathcal{A}^u(\mathscr{P}(T)) \xrightarrow{\;\alpha\;} \mathcal{A}^{sw}(\mathscr{P}(T)) \xrightarrow{\kappa,u,p} \mathcal{A}^{sw}(\check{T}) \overset{\varphi}{\cong} \mathcal{A}^{sw}(T). \qquad (11)$$

Here T stands for an arbitrary tangle in $u\!TT$. The double tree map $\mathscr{P}$ maps T into $sKTG$, and by applying Z^u one obtains a value in $\mathcal{A}^u$, namely a chord diagram on the skeleton of $\mathscr{P}(T)$. We denote the space of chord diagrams on this skeleton by $\mathcal{A}^u(\mathscr{P}(T))$. Now α maps this to arrow diagrams on the skeleton of $\mathscr{P}(T)$, that is, to $\mathcal{A}^{sw}(\mathscr{P}(T))$. In order to revert the skeleton back to that of T, we apply some operations in $\mathcal{A}^{sw}$: a cap attachment κ, unzips and punctures (as shown in Figure 18 and explained below), resulting in a slightly modified version of the desired skeleton, denoted $\check{T}$. Finally, we use that $\mathcal{A}^{sw}(\check{T}) \cong \mathcal{A}^{sw}(T)$ via the sorting isomorphism φ of Lemma 2.5, and hence we obtain a value in $\mathcal{A}^{sw}(T)$, as needed, which, we will later see, is *almost* $Z^w(a(T))$. (Although the punctured strands connect in a single binary tree, VI relations can be used as part of the sorting isomorphism.)

The cap attachment, unzip and puncture operations are done in the order shown in Figure 18. First attach a cap – a capped strand with no arrows on it – to the end of the right vertical strand in $\alpha(\mathscr{P}(T))$: this is a circuit algebra operation in $\mathcal{A}^{sw}$. If T has n ends, perform $(n-1)$ consecutive disc unzips on the capped strand, as shown in Figure 18. Then puncture the left hand tree, for example by puncturing the left vertical strands marked "1, 2,..." in Figure 18 (these punctures also affect the connecting diagonal strands, as in Figure 6). Note that since the punctured tree had originally crossed over the capped tree, these crossings become virtual after puncturing, hence the last equality in Figure 18.

Denote the composition of the maps and operations shown in Equation (11) by ξ, that is,

$$\xi := \varphi \circ p \circ u \circ \kappa \circ \alpha \circ Z^u \circ \mathscr{P} : u\!TT \to \mathcal{A}^{sw}. \qquad (12)$$

Then, $\xi(T) \in \mathcal{A}^{sw}(T)$. We first show that $\xi(T)$ is well-defined, that is, it doesn't depend on the choice of binary trees in $\mathscr{P}(T)$.

Lemma 3.7. *The choice of binary trees in the double tree construction does not affect $\xi(T)$.*
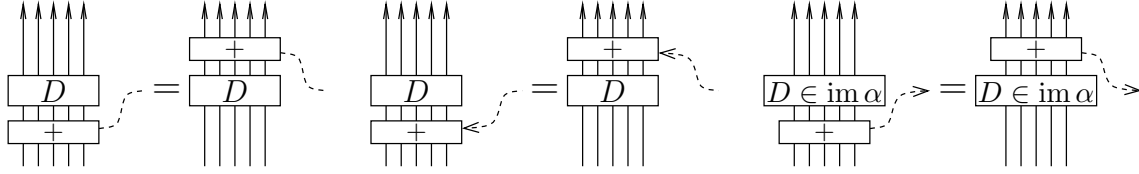
26

Figure 19. The invariance property of chord diagrams on the left, the head invariance and tail invariance properties of arrow diagrams in the middle and right. Here D denotes a chord or arrow diagram on any skeleton; for tail invariance there is a restriction that $D \in \operatorname{im} \alpha$ (with $\alpha : \mathcal{A}^u \to \mathcal{A}^{sw}$). The box labelled "+" denotes a sum of incoming chords or arrows, whose other ends are in the same place. The equalities are understood locally: there may be other skeleton components and chords/arrows elsewhere, which coincide on both sides.

Proof. Any binary tree can be changed into any other binary tree via a sequence of "I to H" moves, as shown on the right. Hence, it is enough to analyze how an I to H move on one of the trees affects the value of $Z^u(\wp(T))$, and prove that the difference vanishes after the caping, unzip, and puncture operations.
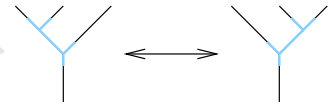
Suppose τ_1 and τ_2 are two binary trees which differ by a single I to H move, and let $\wp_{\tau_1}$ and $\wp_{\tau_2}$ denote the two resulting double-tree maps, assuming the "other side tree" is unchanged. The I to H move can be realised by inserting[16] an associator, followed by unzipping the edge marked '1' on the right, then the edge marked '2'. By the homomorphicity of Z^u, the values $Z^u(\wp_{\tau_2}(T))$ and $Z^u(\wp_{\tau_1}(T))$, only differ in an inserted horizontal chord associator Φ on the three strands involved, we indicate this by writing $Z^u(\wp_{\tau_2}(T)) = Z^u(\wp_{\tau_1}(T)) * \Phi$. If the I to H move was done on the left side tree, then all the strands involved are later punctured, killing any arrow diagram that lived on them by the TF relation. As a result, the only surviving part of Φ is its constant term, 1, and the resulting values of ξ are equal.
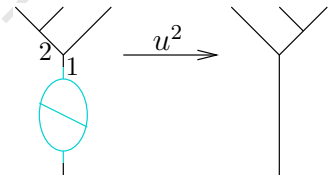
If the I to H move is done on the right side tree, then the all participating strands are capped and disk unzipped. If $\alpha(\Phi)$ is immediately adjacent to the caps, then it cancels by the CP relation. However, it is a priori possible that there are other arrow ending separating Φ from the caps. Note that in $\mathcal{A}^u$, any chord endings can be can be commuted from below the associator to above, using VI relations and the *invariance property* of chord diagrams shown in Figure 19 [BN2, Lemma 3.4]. Thus, one can assume that $\alpha(\Phi)$ is adjacent to the caps and hence cancels. This concludes the proof. $\qquad\square$

There is an action of $\mathbb{Z}/n\mathbb{Z}$ on elements of $u\mathcal{T}T$ with n ends, by cyclic permutations of the ends. The following lemma will be useful later in proving that Z^w is a planar algebra map; we present it now because its proof is similar to that of Lemma 3.7.

Lemma 3.8. *The map ξ is invariant under cyclic permutation of the ends of T.*

Proof. To show that $\xi(T)$ is invariat under cyclic permutations of ends of T, it is enough to show that $\xi(T)$ does not change when the rightmost end of T is moved to the far left (denote this by σT), as shown in Figure 20.

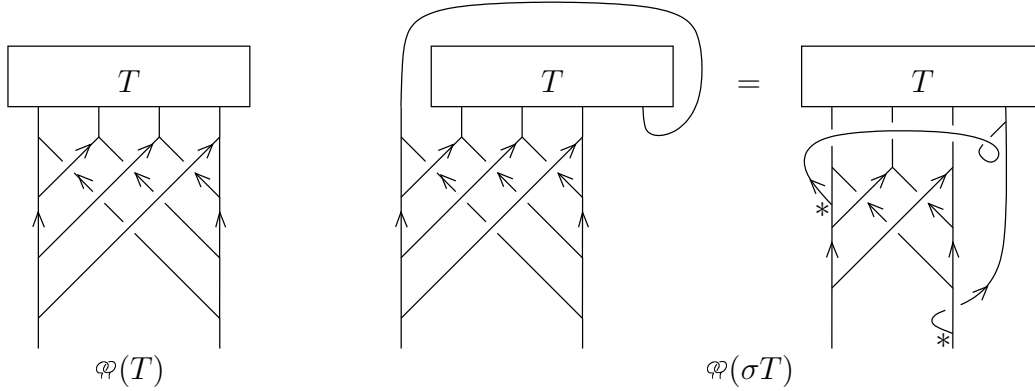[16] See [WKO2, Section 4.6] for a detailed description of the tangle insertion operation in *sKTG*.

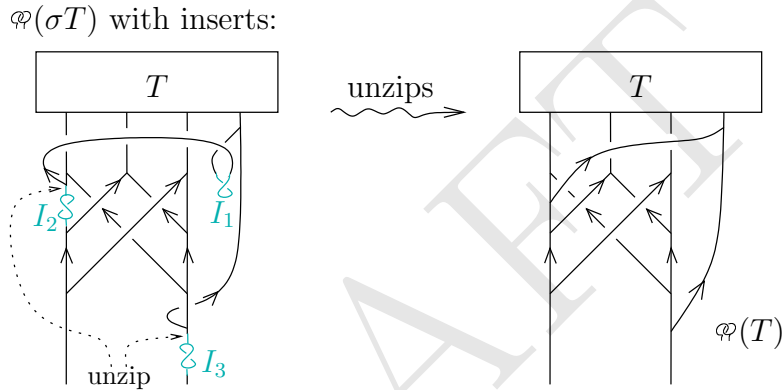**Figure 20.** Double tree construction for cyclically permuted ends of T.

fig:wellde

Figure 21. The difference between $\wp(T)$ and $\wp(\sigma T)$, understood via insertions.

fig:wellde

The rightmost picture of Figure 20 is equivalent as *sKTG*s to $\wp(\sigma T)$. It differs from $\wp(T)$ in three ways:

- the binary trees connecting the ends of T are different;
- two tree branches (marked with $*$ in Figure 20) are connected to the trunk from the opposite side: that is, these trivalent vertices have opposite cyclic orientation;
- one tree branch has a kink in it.

As before, we need to analyse how $Z^u(\wp(\sigma T))$ differs from $Z^u(\wp(T))$, and show that the difference vanishes after the puncture, cap and unzip operations.

To achieve this, we transform $\wp(\sigma T)$ into $\wp(T)$ using tangle insertions. First, cancel the kink by inserting an opposite kink I_1 on the same strand, as shown in Figure 21 in blue[17]. As Z^u is compatible with insertion, the Z^u values will differ by the value of a kink: a chord diagram on the one strand involved. Later in the process this strand is punctured, so the value of the kink cancels by the TF relation.

Similarly, switching the side that the tree branches are attached on amounts to inserting twists I_2 and I_3, and unzipping the connecting edges, also shown in Figure 21. Each of these operations changes the value of Z^u by inserting the value of a twist, which is $e^{c/2}$ for any Z^u, where c denotes a single chord between the appropriate strands [WKO2, Lemma 4.14].
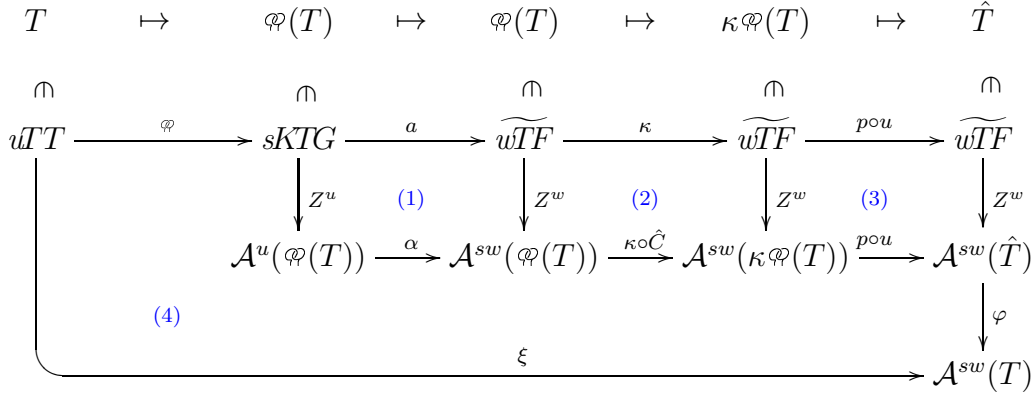
---

[17]Or grey in black and white print.

$$T \quad\mapsto\quad \wp(T) \quad\mapsto\quad \wp(T) \quad\mapsto\quad \kappa\wp(T) \quad\mapsto\quad \hat{T}$$

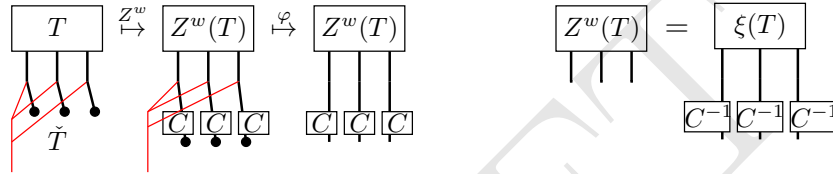**Figure 22.** Compacircle ξ and Z_ξ^w, assuming that Z_ξ^w exists.

Figure 23. Computing $Z_\xi^w(\check{T})$ and $Z_\xi^w(T)$.

Applying α maps this to $e^{(a_L+a_R)/2}$, where a_L and a_R denote horizontal left and right arrows, respectively. On the left side tree, this cancels after punctures, as before. On the right side tree, the strand directly underneath the twist is capped and uzipped, and hence the value of the twist cancels by the CP relation.

Now observe that the right side picture of Figure 21 only differs from $\wp(T)$ in the choices of binary trees, which do not change the value of ξ by Lemma 3.7. $\qquad\square$

The following lemma clarifies the relationship between the map ξ and the (partial) homomorphic expansion Z_ξ^w that we're aiming to construct:

Lemma 3.9. *If there exists a homomorphic expansion Z_ξ^w for $\widetilde{wTF}$ compatible with Z^u, and $T \in uTT$ is a tangle with n ends, then $Z_\xi^w(a(T)) = \xi(T) \cdot (C^{-1})^n$, where $C = Z(\downarrow)$, and $\xi(T)$ is multiplied by C^{-1} at each tangle end of T, as in Figure 23.*

Proof. Assume there exists a homomorphic expansion Z_ξ^w compatible with Z^u. We use, as in Figure 22, the homomorphicity of Z_ξ^w and its compatibility with Z^u to show that $\xi(T) = Z_\xi^w(\check{T})$, where $\check{T}$ is as in Equation 11 and shown in Figure 23 on the left.

If the diagram in Figure 22 commutes, then for any $T \in uTT$ and any Z^u-compatible Z_ξ^w, we have $\varphi(Z_\xi^w(\check{T})) = \xi(T)$. Since Z_ξ^w is a circuit algebra homomorphism, $Z_\xi^w(\check{T})$ can be obtained from $Z_\xi^w(T)$ by attaching the Z_ξ^w-value of a left-punctured right-capped vertex at each tangle end, as illustrated in Figure 23. By Lemma 2.9 we have $Z_\xi^w\big(\text{\scriptsize↗} \big) = 1$, so the only additions are C values at each capped end, as shown in Figure 23. This can then be interpreted as a value in $\mathcal{A}^{sw}(T)$ via the sorting isomorphism φ of Lemma 2.5. This implies the statement of the Lemma.

29

It remains to show that the diagram in Figure 22 commutes. The square (1) is the assumed the compatibility of Z^u and Z^w_ξ. In square (2), recall the map κ denotes the circuit algebra operation of attaching a cap at the bottom right end of the w-foam. The map $\hat{C}$ denotes the circuit algebra operation which attaches a value $C = Z(\downarrow)$ at the end of the strand. Thus, the commutativity of square (2) is implied by the homomorphicity of Z^w_ξ with respect to circuit algebra composition (as a binary operation). The square (3) is commutative due to the homomorphicity of Z^w_ξ with respect to punctures and disc unzips.

The commutativity of the heptagon (4) would be true by definition, if not for the map $\hat{C}$ (multiplication by the cap value). We show that, in fact, the value C cancels after punctures, by a property of arrow diagrams in the image of α, called *tail-invariance*, shown in Figure 19 (see [WKO2], Remark 3.14 and early in Section 3.3). In the current situation tail invariance means that the value C, which has only arrow tails, can be moved from one tangle end to the other, as shown on the right. Consequently, C cancels when the left strand is punctured. $\square$
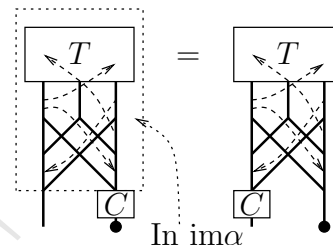
Remark 3.10. In Lemma 3.9 we assume by convention that all tangle ends of T are oriented upwards (towards T). If k tangle ends are oriented down, the corresponding cap values appear with their orientations switched: $Z^w_\xi(aT) = \xi(T) \cdot (C^{-1})^{n-k}(S(C)^{-1})^k$.

Corollary 3.11. *If there exists a homomorphic expansion Z^w for $\widetilde{wTF}$ compatible with Z^u, then $\pi(V) = \pi(\xi(\curlywedge))$, where V is the Z^w-value of the vertex, and π is the tree projection.*

Next, we aim to show that Z^w_ξ is compatible with Z^u. This requires a technical lemma, in which we compute the ξ-value of a vertical strand:

Lemma 3.12. *For a single un-knotted strand, $\xi(\curvearrowright) = \alpha(\nu^{1/2})$, where $\nu \in \mathcal{A}^u(\curvearrowright)$ denotes the Kontsevich integral of the un-knot[18].*

Proof. We apply $\wp$ to $\curvearrowright$, as shown in Figure 24, and comupte $Z^u(\wp(\curvearrowright))$ using the finite generation property of *sKTG* and the homomorphicity of Z^u. In [WKO2, Section 5.2] we gave an algorithm for writing any *sKTG* as an *sKTG*-composition of generators (the primary operation in *sKTG* is *tangle insertion*, see [WKO2, Figure 22]). Feeding $\wp(\curvearrowright)$ into this algorithm, one needs to "curve up" one strand as in Figure 24, in this case the strand on the right (the choice of strand doesn't affect the outcome).

The chord diagram $Z^u(\wp(\curvearrowright))$ is shown in Figure 24, expressed in terms of the generators of *sKTG* described in [WKO2, Proposition 4.13]: the value Φ of the *associator graph*, which is a Drinfel'd associator; the value $R = e^{c/2}$ of the *twist graph*, where c is a single chord; and the values n and b of the *noose* and *balloon* graphs, respectively.

In $\xi(\curvearrowright)$, Z^u is followed by α, a cap attachment, unzips and punctures. As explained in [WKO2, Section 4.6], we have $\alpha(b) = e^{a/2}\alpha(\nu)^{1/2}$, and $\alpha(n) = e^{-a/2}\alpha(\nu)^{1/2}$. Both factors are local arrow diagrams on a single strand and hence commute with all other arrow endings. Hence the exponential part of n cancels by the CP relation, and the wheels part $\alpha(\nu)^{1/2}$ can be moved to the bottom left end by the tail invariance property (as in the last paragraph

---

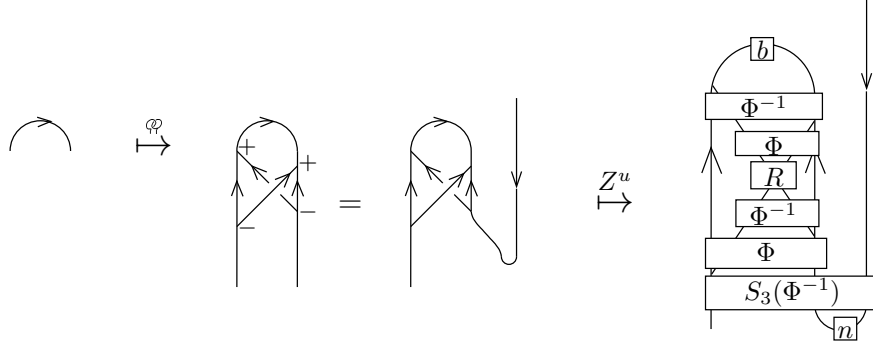[18]The value of ν was conjectured in [BGRT] and proven in [BLT]. Note that ν involves wheels only.

Figure 24. The double tree map composed with Z^u, applied to a single strand. To compute $Z^u(\wp(\curvearrowright))$, we write $\wp(\curvearrowright)$ as a composition of generators; this requires first expressing it as a bottom-top tangle. See [WKO2, Proposition 4.13] for details.
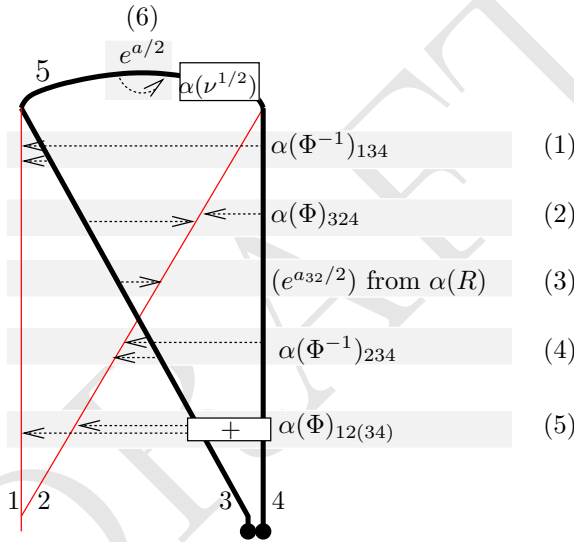

Figure 25. The value of $puk\alpha Z^u\wp(\curvearrowright)$: the numbering (1) through (6) refer to the paragraphs where each component is explained.

of the proof of Lemma 3.9), where it cancels given punctures. Subsequently, the associator $\alpha(S_3(\Phi^{-1}))$ cancels by Fact (3) of Lemma 3.2.

Taking these cancellations into account, the value $puk\alpha Z^u\wp(\curvearrowright) \in \mathcal{A}^{sw}$ is shown in Figure 25 and explained below. Recall that α maps a chord to the sum of its two possible orientations. However, when one supporting strand is punctured, only one of these orientations survive. Hence, for example, $p_2(\alpha(R_{23})) = (e^{a_{32}/2})$. Figure 25 shows a schematic picture of $puk\alpha Z^u\wp(\curvearrowright)$ with exponentials and associators indicated by single arrows. Recall that $\Phi \in \mathcal{A}^{hor}(\uparrow_3)$ can be written as a power series in any two of the three generators of $\mathcal{A}^{hor}(\uparrow_3)$: c_{12}, c_{23} and c_{13}. For example, $\Phi(c_{12}, c_{23}) = \Phi(c_{12}, -c_{12} - c_{23})$. For each associator we chose the presentation in which $puk\alpha(\Phi)$ is of the simplest form.

(1) The top associator of Figure 24, after applying a VI relation, is written as $\Phi^{-1}_{13(24)}$ in the strand numbering of Figure 25. We write this in terms of c_{13} and $c_{1(24)} = c_{12} + c_{14}$.

31

Observe that $p_1\alpha(c_{13}) = a_{31}$ and $p_1p_2\alpha(c_{1(24)}) = a_{41}$, thus

$$p_1p_2\alpha\Phi^{-1}(c_{13}, -c_{13} - c_{1(24)}) = \Phi^{-1}(a_{31}, -a_{31} - a_{41}).$$

This is reflected in Figure 25 in drawing only the a_{31} and a_{41} arrows. Now note that by the VI relation at the top right vertex, $a_{41} = -a_{51}$. The local arrow diagrams $e^{a/2}$ and $\alpha(\nu^{1/2})$ on strand 5 commute with arrow tails, and therefore a_{51} can be pulled to the left, where by another VI relation, $a_{41} = -a_{51} = -a_{31}$. Thus, $\Phi^{-1}(a_{31}, -a_{31} - a_{41}) = \Phi^{-1}(a_{31}, 0) = 1$. Note the similarity to Fact (3) of Lemma 3.2.

(2) Second from top, by the same argument, we have

$$p_1p_2\alpha(\Phi_{324}) = p_1p_2\alpha(\Phi(c_{23}, c_{24})) = \Phi(a_{32}, a_{42}) = \Phi(a_{32}, -a_{32}) = 1.$$

(3) For the exponential,

$$p_1p_2\alpha(R_{23}) = p_1p_2\alpha(e^{c_{23}/2}) = e^{a_{32}/2}.$$

(4) Using the same reasoning again,

$$p_1p_2\alpha(\Phi_{234}^{-1}) = p_1p_2\alpha(\Phi^{-1}(c_{23}, -c_{23} - c_{24})) = \Phi^{-1}(a_{32}, -a_{32} - a_{42}) = \Phi^{-1}(a_{32}, 0) = 1.$$

Note that here we use that the arrow tail of a_{32} commutes with the arrow tails of the exponential.

(5) By Fact (2) of Lemma 3.2,

$$p_1p_2\alpha(\Phi)_{12(34)} = 1.$$

(6) Finally, move the top exponential $e^{a/2}$ to strands 3 and 2, using the VI relation at both vertices. At the top left vertex, the arrow tails move freely from strand 5 to strand 3. The heads commute with $\alpha(\nu)$, and at the top right vertex they are killed on strand 4 due to the CP relation, and on strand 2 they acquire a negative sign due to opposite orientations. Hence, $(e^{a_{55}/2}) = (e^{-a_{32}/2})$, and this cancels $\alpha(R)$.

In summary, $\xi(\frown) = \alpha(\nu^{1/2})$, as claimed. $\qquad\square$

As an aside, Lemma 3.12 enables a quick computation of the even part of $C = e^c = Z_\xi^w(\downarrow)$. Recall that c is a linear combination of wheels: $c = \sum_{n=2}^\infty \gamma_n w_n$. Let $c = c_0 + c_1$, where c_0 denotes the even part of c (sum of all even wheels), and c_1 denotes the odd part, that is, $c = c_0 + c_1$. Let $C_0 = e^{c_0}$, the even part of C. Corollary 3.13 below shows in particular that the even part of the C is independent of the choice of Z^b (that is, the choice of Drinfel'd associator) and Z^u.

Corollary 3.13. *If $C = Z_\xi^w(\downarrow)$, and C_0 is the even part of C, then $C_0 = \alpha(\nu^{1/4})$, regardless of the choice of expansion Z^u used to construct Z_ξ^w.*

Proof. By Lemma 3.9 and Remark 3.10, we have $Z_\xi^w(\frown) = C^{-1}\xi(\frown)S(C^{-1})$. Note that $S(w_{2k}) = w_{2k}$ and $S(w_{2k+1}) = -w_{2k+1}$, and hence $S(C) = e^{c_0-c_1}$. Also, by homomorphicity, $Z_\xi^w(\frown) = 1$. Thus, by Lemma 3.12, $1 = e^{c_0+c_1}\alpha(\nu^{1/2})e^{c_0-c_1}$, and therefore $\alpha(\nu^{1/2}) = e^{2c_0}$, which gives $C_0 = e^{c_0} = \alpha(\nu^{1/4})$.

Next we prove that Z_ξ^w is indeed compatible with Z^u:

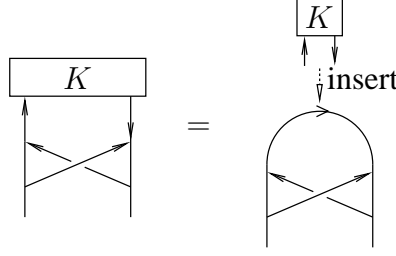**Proposition 3.14.** *For any $K \in sKTG$, $Z_\xi^w(a(K)) = \alpha(Z^u(K))$.*

32

Figure 26. For $K \in sKTG$, $\wp(K)$ is K inserted into $\wp(\frown)$.

Proof. Note that $sKTG \subseteq uTT$, and for $K \in sKTG$, $\wp(K)$ can be obtained by inserting K into the top strand of $\wp(\frown)$: see Figure 26. Since Z^u is compatible with insertions, $Z^u(\wp(K))$ can be obtained by $Z^u(K)$ inserted into $Z^u(\wp(\frown))$. Through the sequence of α, capping, puncturing, φ and multiplications by C^{-1}, all of $Z^u(\wp(\frown))$ cancels, as in Lemma 3.12. Note that the cancellations still go through despite the fact that $\alpha(Z^u(K))$ is inserted on the top strand: this follows from the fact that $\alpha(Z^u(K))$ is in the α-image of $\mathcal{A}^u$, and the appropriate "commutativity" property holds in $\mathcal{A}^u$. Hence, $Z^w_\xi(K) = Z^w_\xi(K)$ as required. $\qquad\square$

Now, we show that Z^w_ξ it is a planar algebra homomorphism on $a(uTT)$. This is technically challenging, but it implies the R4 equation immediately. For the proof, it will be necessary to know the behaviour of Z^u with respect to edge deletions. When an edge e of a knotted trivalent graph $K \in sKTG$ is deleted, the two vertices at each end of e cease to be vertices. The associated graded operation on chord diagrams deletes skeleton edge e, and chord diagrams with any chord endings on e are set equal to 0.

Fact 3.15. *Z^u commutes with edge deletions up to a possible correction term of $e^{\pm c/4}\nu^{1/2}$ depending on the position of the edge, as in Figure 27.*

Proof sketch. In [WKO2, Section 4.6.1] Z^u is constructed from an invariant Z^{old} by adding vertex normalizations, as shown in Figure 27. Note that the top two diagrams in the figure differ from [WKO2, Figure 29] in a single edge orientation switch, which switches the vertex sign and accordingly the normalization[19]. In fact, Z^{old} commutes with edge deletions [Da, Proposition 6.7], so the edge deletion error (and hence, the correction term) for Z^u arises from the vertex normalisations implemented, as shown in Figure 27. $\qquad\square$

Remark 3.16. There is also an "edge delete" operation of $\widetilde{uTF}$: this is not required for the finite presentation of $\widetilde{uTF}$ or $\mathcal{A}^{sw}$, but it is necessary for the proof of Theorem 3.17 below. When deleting an edge in $\widetilde{uTF}$ – which can be either a tube or a string – the vertices at either end[20] cease being vertices. The associated graded operation $d_e : \mathcal{A}^{sw} \to \mathcal{A}^{sw}$ deletes the skeleton edge e and sends any arrow diagram with arrow endings on the deleted strand to zero. The crucial fact we need is that edge delete operations for chord and arrow diagrams

---

[19]The point of the normalization is to make Z^u commute with unzips. The reader might wonder, why normalize so that the expansion respects unzips, rather than deletions? The answer is that for finite generation of knotted trivalent graphs, unzips are crucial but deletions are not.

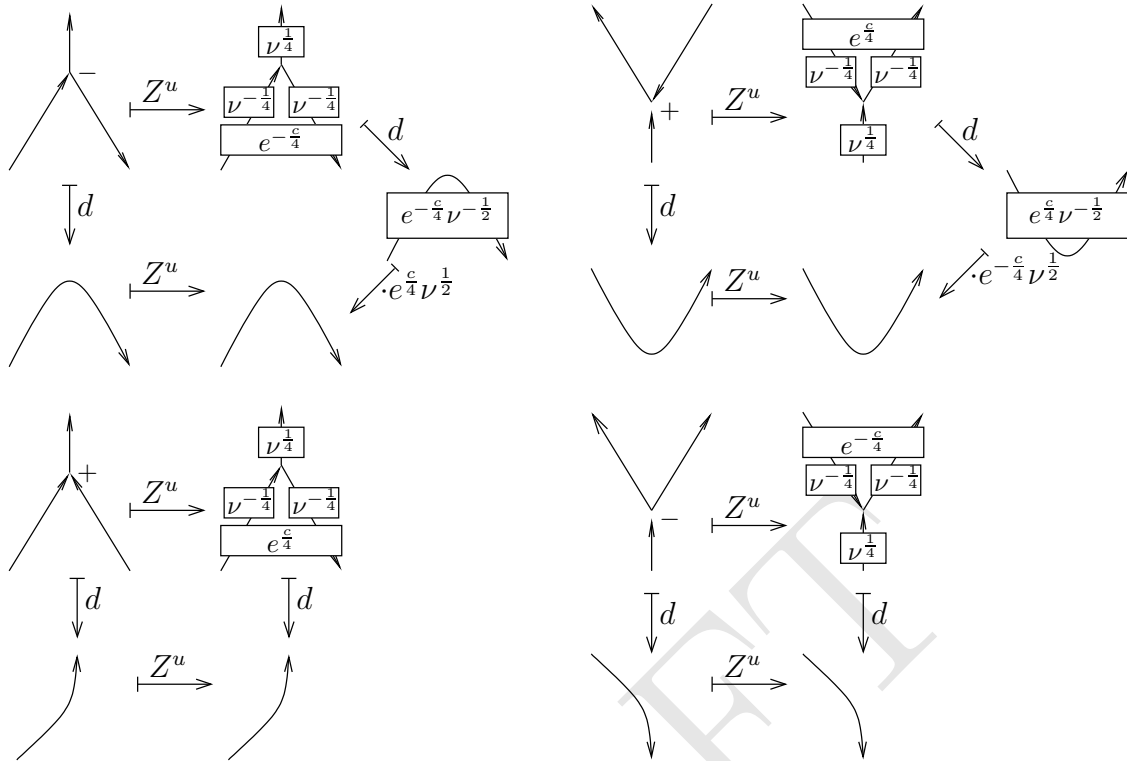[20]It is also possible to delete a capped edge.

Figure 27. In [WKO2, Section 4.6.1] Z^u is constructed from an invariant Z^{old} by applying vertex normalizations, which depend on vertex signs: these are shown along the top horizontal arrow of each diagram (see also [WKO2, Figure 29]). It follows Z^u is only homomorphic up to a correction term when deleting the top edge of a positive vertex (first in the total ordering around the vertex) or the bottom edge of a negative vertex: see the top two diagrams. In other edge deletions the normalizations cancel, and hence Z^u is homomorphic with respect to these edge deletions, as for example in the bottom two diagrams.

fig:ZuDele

are compatible via the map α, which is immediate from the definitions:

$$
\begin{array}{ccc}
\mathcal{A}^u & \xrightarrow{\ \alpha\ } & \mathcal{A}^{sw} \\
\downarrow{\scriptstyle d_e} & & \downarrow{\scriptstyle d_e} \\
\mathcal{A}^u & \xrightarrow{\ \alpha\ } & \mathcal{A}^{sw}
\end{array}
$$

thm:PAMap **Theorem 3.17.** *The map Z^w_ξ is a planar algebra map on $a(uTT)$.*

Proof. Planar algebra operations can be written as compositions of two simpler, basic operations: disjoint unions and contractions. In the disjoint union of two tangles T_1 and T_2, the ends of $T_1 \sqcup T_2$ are ordered by declacircle that the ordered ends of T_1 come first, followed by the ordered ends of T_2. The contraction operation c_i applies to any tangle with at least $i + 1$ ends: it acts by joining the i-th and $(i + 1)$-st ends of T and re-numbering the rest, resulting in a tangle with two ends less. Both operations are shown in Figure 28.
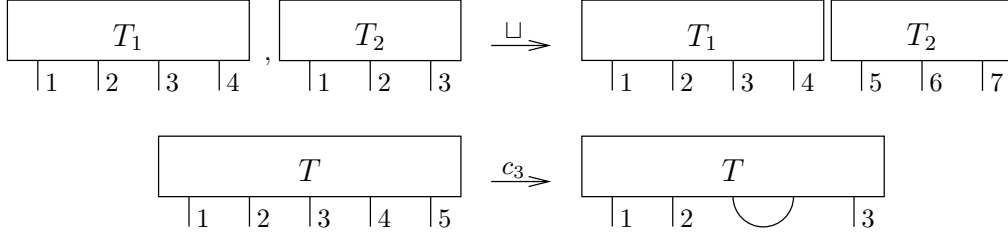
fig:AtomicPAOps

34

Figure 28. Basic planar algebra operations: disjoint union and contraction.
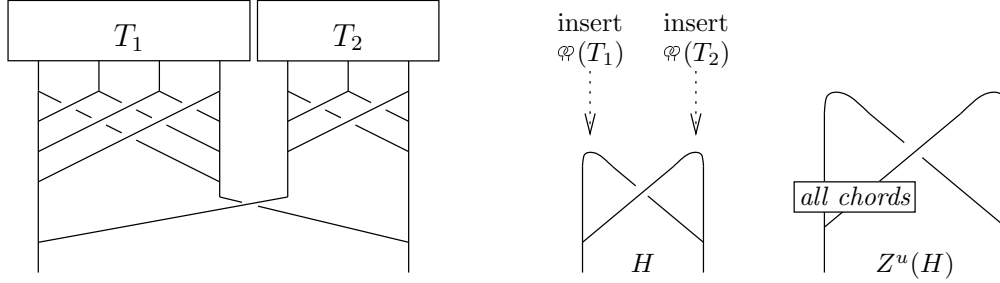
Figure 29. The double tree map applied to a disjoint union of $u\!TT$-s is the same as inserting the double tree of each individual $u\!TT$ into the $sKTG$ H. In $Z^u(H)$ all chords can be pushed into the rectangle shown, using VI relations when necessary.

Thus, we only need to show that Z_ξ^w commutes with these two operations, that is, $Z_\xi^w(T_1 \sqcup T_2) = Z_\xi^w(T_1) \sqcup Z_\xi^w(T_2)$, and $Z_\xi^w(c_i(T)) = c_i(Z_\xi^w(T))$. Note that the right sides of these equalities make sense: arrow diagrams on the skeleta of $a(u\!TT)$, where Z_ξ^w takes values, also form a planar algebra, and in particular disjoint union and concatenation of arrow diagrams is well defined.

Disjoint unions. We need to compute $\xi(T_1 \sqcup T_2)$, where $T_1, T_2 \in u\!TT$. The value $\wp(T_1 \sqcup T_2)$ is shown in Figure 29. The binary trees in $\wp$ can be chosen arbitrarily by Lemma 3.7: Figure 29 shows the most convenient trees for this proof.

Observe that $\wp(T_1 \sqcup T_2)$ can be obtained as an $sKTG$ by inserting $\wp(T_1)$ and $\wp(T_2)$ into a simpler $sKTG$, denoted H, as shown in the same figure (up to orientation switches which don't impact what follows and will be ignored). Hence, $Z^u(\wp(T_1 \sqcup T_2))$ is given by inserting $Z^u(\wp(T_1))$ and $Z^u(\wp(T_2))$ into $Z^u(H)$.

One could compute $Z^u(H)$ explicitly using the same algorithm as before, but we can avoid this work, as follows. All chords in $Z^u(H)$ can be assumed to be located in the rectangle shown in Figure 29 (using VI relations, if necessary). Ducircle the computation of ξ both supporting strands are punctured, and therefore $p^2\alpha(Z^u(H)) = 1$. This implies that $\xi(T_1 \sqcup T_2) = \xi(T_1) \sqcup \xi(T_2)$, and it follows via Lemma 3.9 that $Z_\xi^w(T_1 \sqcup T_2) = Z_\xi^w(T_1) \sqcup Z_\xi^w(T_2)$.

Contractions. Proving that Z_ξ^w commutes with contractions is more involved. By Lemma 3.8, we can assume that the ends contracted are the last (rightmost) two ends of the n ends of T. Hence we will drop the subscript from c_i and denote this operation simply by c.

We need to show that $Z_\xi^w(cT) = cZ_\xi^w(T)$, for any $T \in u\!TT$. Since Z_ξ^w is given by the composition of many maps, this can be restated as the commutativity of the perimeter of a
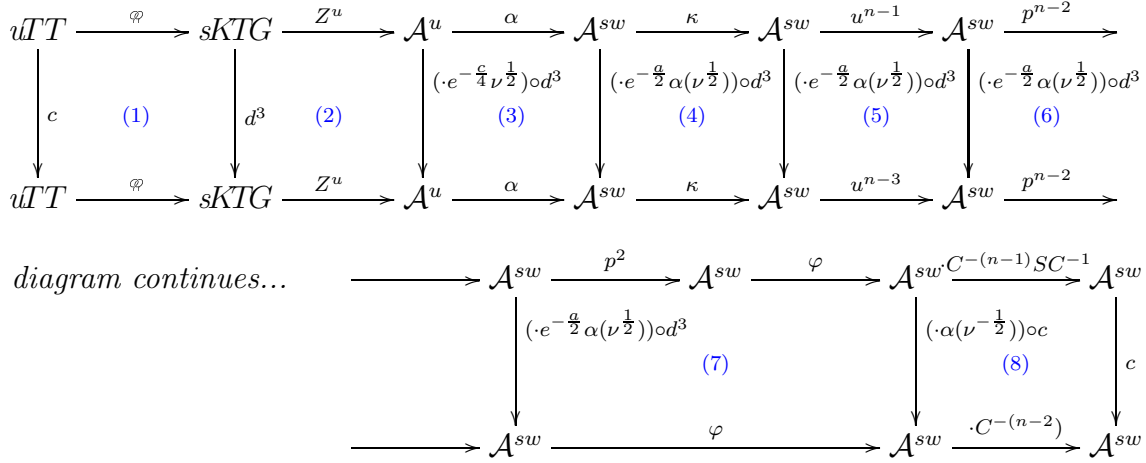
35

$$u\mathbb{T}T \xrightarrow{\;\wp\;} sKTG \xrightarrow{\;Z^u\;} \mathcal{A}^u \xrightarrow{\;\alpha\;} \mathcal{A}^{sw} \xrightarrow{\;\kappa\;} \mathcal{A}^{sw} \xrightarrow{\;u^{n-1}\;} \mathcal{A}^{sw} \xrightarrow{\;p^{n-2}\;}$$

$$\left\downarrow c\quad (1)\qquad \right\downarrow d^3 \quad (2)\qquad \left\downarrow(\cdot e^{-\frac{c}{4}}\nu^{\frac12})\circ d^3 \atop (3) \quad \left\downarrow(\cdot e^{-\frac{a}{2}}\alpha(\nu^{\frac12}))\circ d^3 \atop (4)\quad \left\downarrow(\cdot e^{-\frac{a}{2}}\alpha(\nu^{\frac12}))\circ d^3 \atop (5)\quad \left\downarrow(\cdot e^{-\frac{a}{2}}\alpha(\nu^{\frac12}))\circ d^3 \atop (6)$$

$$u\mathbb{T}T \xrightarrow{\;\wp\;} sKTG \xrightarrow{\;Z^u\;} \mathcal{A}^u \xrightarrow{\;\alpha\;} \mathcal{A}^{sw} \xrightarrow{\;\kappa\;} \mathcal{A}^{sw} \xrightarrow{\;u^{n-3}\;} \mathcal{A}^{sw} \xrightarrow{\;p^{n-2}\;}$$

$$\text{diagram continues...} \qquad \longrightarrow \mathcal{A}^{sw} \xrightarrow{\;p^2\;} \mathcal{A}^{sw} \xrightarrow{\;\varphi\;} \mathcal{A}^{sw} \xrightarrow{\;\cdot C^{-(n-1)}SC^{-1}\;} \mathcal{A}^{sw}$$

$$\left\downarrow(\cdot e^{-\frac{a}{2}}\alpha(\nu^{\frac12}))\circ d^3 \atop (7) \qquad\qquad \left\downarrow(\cdot\alpha(\nu^{-\frac12}))\circ c \atop (8)\qquad \left\downarrow c$$

$$\longrightarrow \mathcal{A}^{sw} \xrightarrow{\;\varphi\;} \mathcal{A}^{sw} \xrightarrow{\;\cdot C^{-(n-2)}\;} \mathcal{A}^{sw}$$

Figure 30. Summary of the proof that Z^w_ξ commutes with contractions: Z^w_ξ is the composition along the entire top and entire bottom horizontal edge of the diagram.

large diagram (shown in Figure 30), which in turn can be broken down to its smaller parts. Throughout this proof, let $T \in u\mathbb{T}T$ denote an arbitrary trivalent tangle.

Square (1). This square (shown schematically on the right) plays out in $u\mathbb{T}T$ and $sKTG$, and commutes by inspection, as shown on the right. The three strands to be deleted are indicated by broken lines. Therefore, $d^3\wp(T) = \wp c(T)$.

Square (2). Square (2) is also on the right: for the Z^u-values skeleta are indicated but chords are not shown. To prove that square (2) commutes, we use the properties of Z^u with respect to deleting edges in $sKTG$, as stated in Fact 3.15 and Figure 27.

Only one of the three edge deletions requires a correction term: this is the edge marked with $*$ in the diagram on the left. This edge ends in a $e^{-c/4}\nu^{1/2}$ inserted at the place of the vertex, where c stands for a single chord. In square (2), this correction term appears at the bottom right corner of the square, where the two ends of T are contracted (see in the diagram showing skeleta in Figure 30). In summary: $\left(d^3 Z^u\wp(T)\right) \cdot (e^{-\frac{c}{4}}\nu^{\frac12}) = Z^u\wp c(T)$.

Square (3). Square (3) is essentially the commutativity of edge deletions stated in Remark 3.16, combined with applying α to the correction term. So we have $\left(d^3\alpha Z^u\wp(T)\right) \cdot (e^{-\frac{a}{2}}\alpha(\nu^{\frac12})) = \alpha Z^u\wp c(T)$.

Square (4). Squares (4), (5), and (6) are shown in detail in Figure 31. Square (4) plays out in $\mathcal{A}^{sw}$ and it is commutative as the deletions and the cap attachments (denoted by κ) affect different strands: see the diagram on the right. Therefore, $\left(d^3\kappa\alpha Z^u\wp(T)\right) \cdot (e^{-\frac{a}{2}}\alpha(\nu^{\frac12})) = \kappa\alpha Z^u\wp c(T)$.
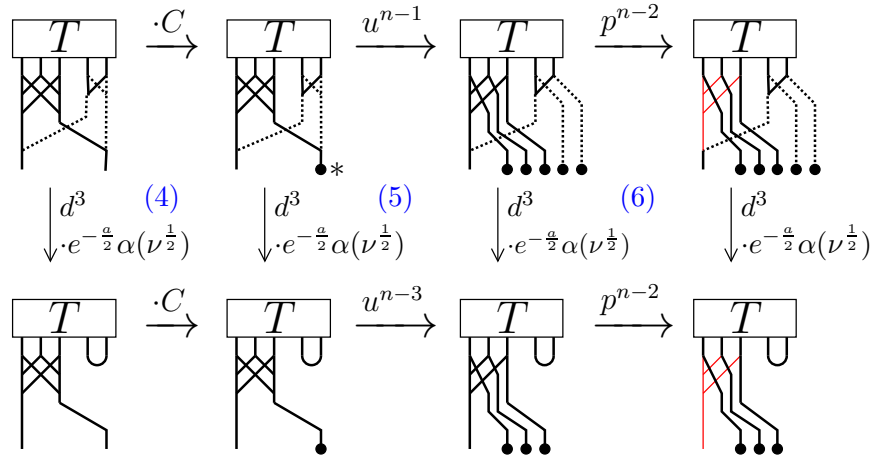
36
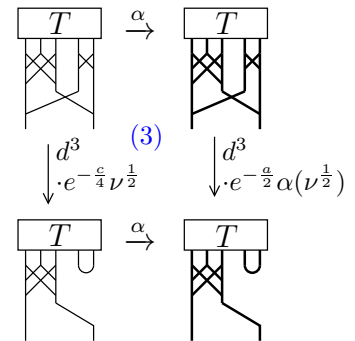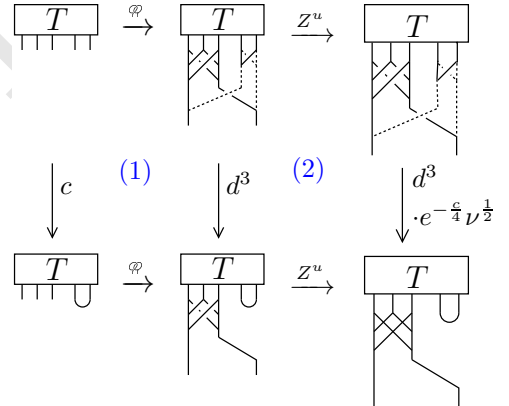
Figure 31. The squares (4) (5) and (6). Strands to be deleted are drawn in dashed lines throughout. The $*$ denotes a cap of interest: see the proof paragraph on square (5).

Square (5). The only difference between $d^3 \circ u^{n-1}$ and $u^{n-3} \circ d^3$ is what happens to arrows on the caped skeleton edge marked by $*$ in Figure 31. Following the diagram right and down, this edge is unzipped $n-1$ times, then the last two of its daughter edges are deleted. On the other hand, following the diagram down and right, the same edge is unzipped $n-3$ times. The results of these compositions are the same by definition of the unzip and delete operations. Thus, we have

$$\left(d^3 u^{n-1} \kappa \alpha Z^u \wp(T)\right) \cdot \left(e^{-\frac{a}{2}} \alpha(\nu^{\frac{1}{2}})\right) = u^{n-3} \kappa \alpha Z^u \wp c(T).$$

Square (6). The deletions and punctures occur on different strands, as shown in Figure 31, hence these operations commute commute. One detail to note is that when a tube strand is deleted at a "tube-and-string" vertex, all that is left is a string (as in the case of puncturing the tube at a tube-string vertex, see Figure 6). In summary:

$$\left(d^3 p^{n-2} u^{n-1} \kappa \alpha Z^u \wp(T)\right) \cdot \left(e^{-\frac{a}{2}} \alpha(\nu^{\frac{1}{2}})\right) = p^{n-2} u^{n-3} \kappa \alpha Z^u \wp c(T).$$
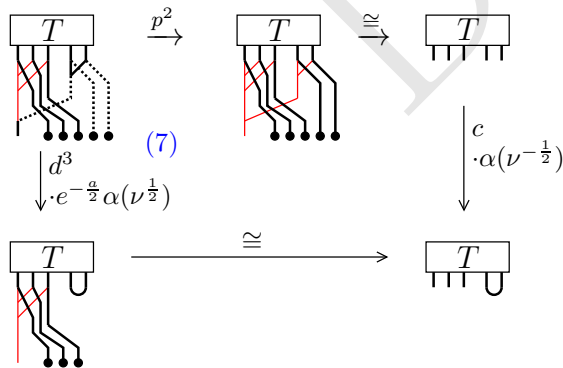
Pentagon (7). The pentagon (7) is shown on the left. This is the most delicate part of the proof. We first show that – for the specific input of $p^{n-2} u^{n-1} \kappa \alpha Z^u \wp(T)$ – the pentagon (7) commutes up to a single possible multiplicative error on the contracted (u-shaped) strand, and later prove that this error is necessarily 1.

To begin, a better understanding of the arrow diagram $p^{n-2} u^{n-1} \kappa \alpha Z^u \wp(T)$ in the top left corner is necessary. All of the operations performed on T, with the exception of Z^u, are "easy" in the sense that we have a complete understanding of their effect. Z^u is "hard", but we can compute the relevant part of its value using the finite generation of *sKTG* ([WKO2, Proposition 4.13]). The computation is shown in Figures 32 and 33 and their captions.

In summary, $Z^u(\wp(T))$ is given by inserting $Z^u(A)$ into the chord diagram D of Figure 33. Now we need to analyze what happens when one applies α, the cap attachment, unzips and
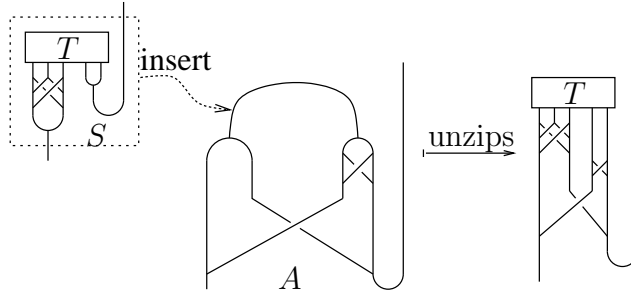
37

Figure 32. Computing the top left corner of Square 7, Step 1: $\mathscr{P}(T)$ can be expressed as the *sKTG* denoted S inserted into the *sKTG* denoted A, followed by unzips, as shown. Z^u respects insertions, hence computing $Z^u(A)$ determines the value of $Z^u(\mathscr{P}(T))$ outside of S.

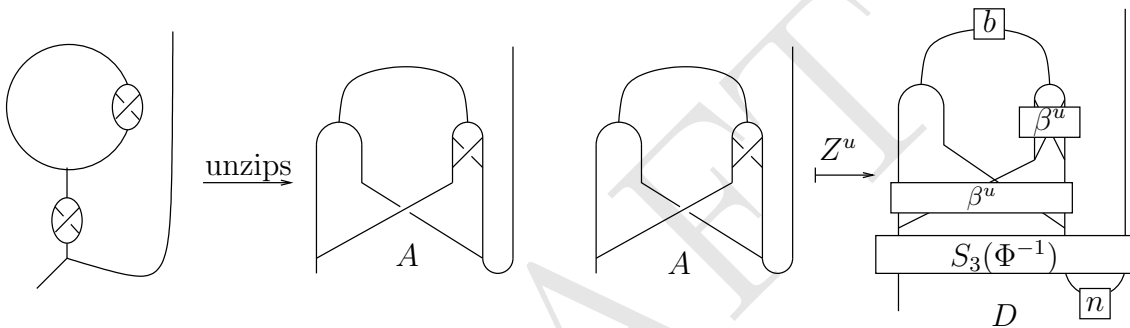fig:Square

Figure 33. Computing the top left corner of Square 7, Step 2: computing $Z^u(A)$. The *sKTG* A can be obtained by inserting the *buckle sKTG* twice into a simpler *sKTG*, and unzipping, as shown on the left. The value of the buckle was computed in Figure 15. Using this value—denoted β^u—and the algorithm in [WKO2, Section 5.2], one computes $Z^u(A)$. The result is denoted D and shown on the right.

fig:Square

punctures to this value: this is an exercise similar to what has been done for Lemma 3.12. The result is shown in Figure 34, and explained below. First note that the n value in D of Figure 33 cancels after punctures by the tail-invariance property (Figure 19), as in the last paragraph of the proof of Lemma 3.9; so does the bottom Φ^{-1} in D, by Fact (3) of Lemma 3.2. These components are not shown in Figure 34.

Working downwards from the top left of the pentagon in Figure 34, the three edge deletions cancel both buckle (β^w) values. The value b value at the top of the diagram D is pulled down across the vertex using a VI relation: this has the same effect as an unzip and an orientation switch on the second stand (as this is oriented downwards). The resulting value $S\alpha u(b)$ cancels by the following reasoning – essentially by definition of unzips and orientations switches – which is illustrated in Figure 35:

Given an arrow 'a' ending on strand 'e', unzipping e produces a sum of two arrows $a_1 + a_2$: one ending on each daughter strand. Reversing the orientation of the first daughter strand gives $-a_1 + a_2$. Contracting the two daughter strands to form a U-shape identifies a_1 and a_2, making $a_1 - a_2$ vanish.
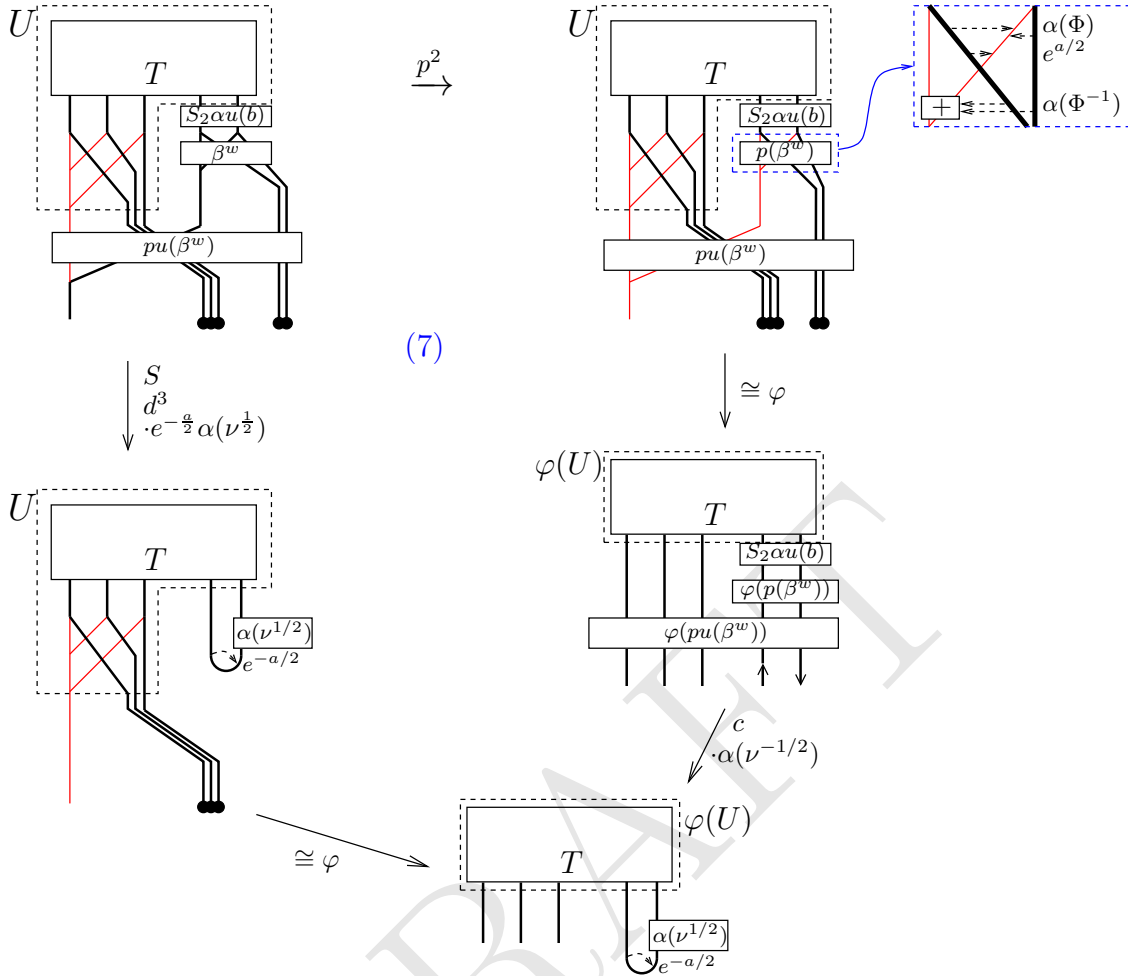
38

Figure 34. The more detailed picture of the pentagon 7.
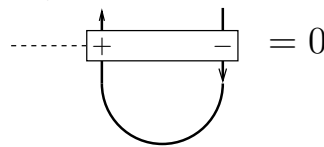

$$---\!\!---\boxed{+ \quad -} \; = 0$$

Figure 35. Unzip, switch orientation and connect kills arrows on the strand.

This is exactly what happens to the arrow diagram $S_2\alpha u(b)$ (just under the tangle T in Figure 34) after the edge deletions or contraction, hence this component cancels it in both directions of the pentagon (7).

The bottom arrow on the left is the Sorting Isomorphism φ of Lemma 2.5.

On the other hand, working from the top left corner of the pentagon (7) to the right: from Section 3.2, using the strand numbering convention of Figure 16, we have

$$p_1 p_3 \beta^w = \Phi^{-1}(a_{2(13)}, -a_{2(13)} - a_{4(13)}) \cdot e^{a_{23}/2} \cdot \Phi(a_{23}, a_{43}).$$

This is shown in the enlarged rectangle at the top right corner of Figure 34. The same is true for $pu(\beta^w)$ at the bottom, except with more unzips.
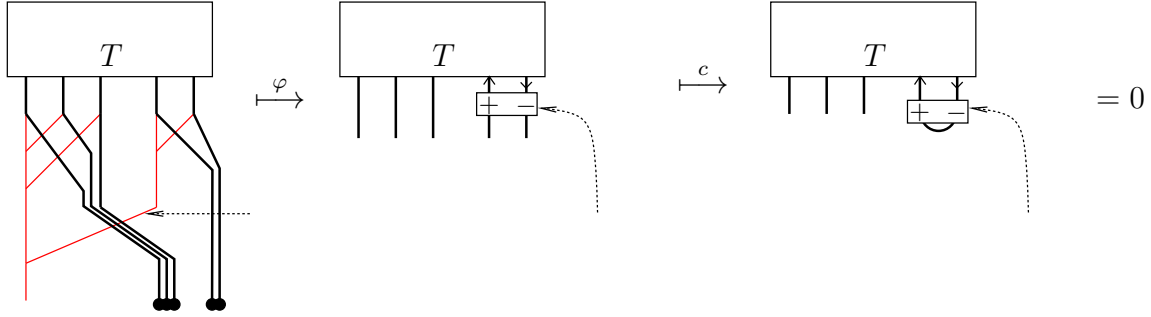
39

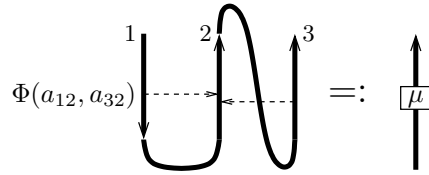**Figure 36.** The cancellation of $\varphi(pu(\beta^w))$.

$$\Phi(a_{12}, a_{32}) \dashrightarrow \quad =: \quad \boxed{\mu}$$

Figure 37. The Φ component of $\varphi(p(\beta^w))$ after contraction.

From here, the first downward arrow applies the Sorting Isomorphism φ of Lemma 2.5, followed by the contraction and correction term along the second downward arrow. At the bottom of the diagram, $\varphi(pu(\beta^w))$ cancels altogether after contraction, in a similar fashion to Figure 35. Namely, φ and the contraction annihilates any arrow ending on the diagonal red strand, or the double capped strand on the right, as shown in Figure 36 for the diagonal red strand. This cancels each factor of $pu(\beta^w)$.

Of the top $\varphi(p(\beta^w))$ shown in the enlarged rectangle, the Φ^{-1} component cancels by the same contraction argument; only the exponential and the Φ component remains. The arrow in the exponent of $e^{a/2}$ switches sign due to the reversed orientation: this is the $e^{-a/2}$ component at the bottom of the pentagon in Figure 34. After contraction, the Φ component gives rise to a "local" arrow diagram on a single strand shown in Figure 37 and denoted μ.

In summary, we see that the pentagon (7) commutes if and only if $\mu = \alpha(\nu)$, and otherwise commutes up to a localised error on the contracted strand, of value $\alpha(\nu)^{-1}\mu$.
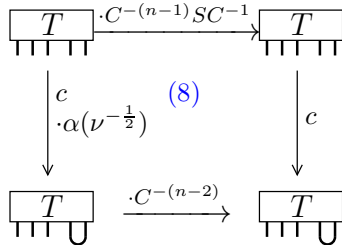
Square (8). Finally, for square (8) we need to check that $C^{-1}S(C^{-1}) = \alpha(\nu^{-1/2})$. Note that the orientation switch negates odd wheels and preserves even wheels, therefore in $C^{-1}S(C^{-1})$ the odd part of C^{-1} cancels, and $C^{-1}S(C^{-1}) = C_0^{-2} = \alpha(\nu^{-1/2})$ by Corollary 3.13. This verifies Square (8).

We have therefore shown that Z^w commutes with contraction up to an error $\alpha(\nu)^{-1}\mu$ on the contracted strand. It remains to show that this error is 1. This follows from the facts that $Z^w(\uparrow) = 1$, and that Z^w commutes with disjoint unions:

$$1 = c(Z^w(\uparrow\downarrow)) = \alpha(\nu)^{-1}\mu Z^w(c(\uparrow\downarrow)) = \alpha(\nu)^{-1}\mu \cdot Z^w(\frown) = \alpha(\nu)^{-1}\mu.$$

This completes the proof. $\qquad\qquad\square$
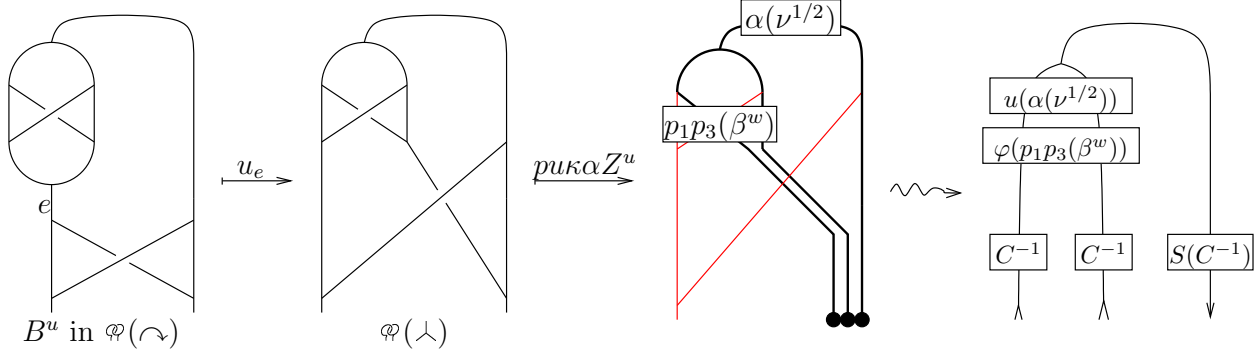
40

Figure 38. On the left we show how to obtain $\mathscr{P}(\curlywedge)$ via an unzip from B^u inserted into $\mathscr{P}(\frown)$. From this we compute $\xi(\curlywedge)$, and finally V on the right.

Note that as a side result we have proven the following curious fact about associators:

Proposition 3.18. *For any Φ horizontal chord associator, μ defined from Φ as in Figure 37, and ν the Kontsevich integral of the unknot, $\mu = \alpha(\nu)$ in $\mathcal{A}^{sw}$.* $\square$

The value $V = Z_\xi^w(\mathcal{J}_\kappa)$ differs, on first glance, from the value V_β constructed in Section 3.1. In the next lemma we show that in fact $V = V_\beta$: this serves both as a reality check, and as a technical tool for showing – in Theorem 3.22 – that Z_ξ^w satisfies the Cap equation.

Lemma 3.19. *The two vertex values from the buckle and the double tree constructions coincide: $V_\beta = V$.*

Proof. Notice that $\mathscr{P}(\curlywedge)$ – as in Figure 38 – can be obtained from simpler *sKTG*s by inserting the buckle B^u into $\mathscr{P}(\frown)$ followed by an unzip. We computed $\xi(\frown)$ in Lemma 3.12. Since Z^u is compatible with insertions and unzips, $Z^u(\curlywedge)$ can be computed by inserting the buckle value β^u (computed in Section 3.2) into $Z^u(\mathscr{P}(\curlywedge))$.

To compute $\xi(\curlywedge)$ we then apply α and the cap, unzip and puncture operations. Because $\beta^w = \alpha(\beta^u)$ is local (is confined to the skeleton of the inserted B^u graph) and is in the image of α, all other arrow endongs commute with it by the head- and tail-invariance properties of $\mathcal{A}^{sw}$ (Figure 19). Therefore, all of the cancellations in the computation of $\xi(\frown)$ still occur, and $\xi(\curlywedge)$ is as shown in Figure 38. Writing this in $\mathcal{A}^{sw}(\uparrow_2)$ we obtain $\varphi(p_1 p_3(\beta^w)) u(\alpha(\nu^{1/2}))$.

To obtain $V = Z_\xi^w(\mathcal{J}_\kappa)$, one multiplies $\xi(\curlywedge)$ at each end by C^{-1} or $S(C^{-1})$ depending on orientation, as shown in Figure 38 on the right. Thus,

$$V = C_1^{-1} C_2^{-1} \varphi(p_1 p_3 \beta^w) u(\alpha \nu^{1/2}) u(S(C^{-1}).$$

On the other hand, from Section 3.2, we have:

$$V^\beta = C_1^{-1} C_2^{-1} \varphi(p_1 p_3 \beta^w) u(C).$$

Thus, we need to show that:

$$C_1^{-1} C_2^{-1} \varphi(p_1 p_3 \beta^w) u(\alpha \nu^{1/2}) u(S(C^{-1}) = C_1^{-1} C_2^{-1} \varphi(p_1 p_3 \beta^w) u(C),$$

in $\mathcal{A}^{sw}(\uparrow_2)$. Multiplying with $(\varphi(p_1 p_3 \beta^w)))^{-1} C_1 C_2$ on the left (bottom) and by $u(S(C))$ on the right (top), this simplifies:

$$u(\alpha \nu^{1/2}) = u(C) u(S(C)).$$

41

Since unzips commute with orientation switches, it is sufficient to prove that

$$CS(C) = \alpha(\nu^{1/2}).$$

Recall that in $CS(C)$ all odd wheels cancel, hence $CS(C) = (C_0)^2$, where C_0 denotes the even part of C. Indeed, by Corollary 3.13, $C_0^2 = \alpha(\nu^{1/2})$. $\qquad\square$

Corollary 3.20. *The "buckle" amd "double tree" constructions lead to the same result, that is, $Z_\xi^w = Z_\beta^w$.*

Proof. Since any homomorphic expansion Z^w of $\widetilde{uTF}$ is uniquely determined by $Z^w(\lambda_\kappa)$, this is immediate from Lemma 3.19. $\qquad\square$

The next lemma implies that V satisfies the Unitarity (U) equation:

Lemma 3.21. *The map Z_ξ^w commutes with strand unzips in uTT.*

Proof. We first note that in uTT unzip is only defined for internal edges, that is, edges which end in a vertex[21] at both ends. By construction, Z_ξ^w is a composition of several maps. We show that edge unzips commute with every one of these, hence with Z_ξ^w.

The $\wp$ map involves only the tangle ends, which are unchanged by unzipping an internal strand, hence these operations commute. The homomorphic expansion Z^u commutes with edge unzips, as shown in [WKO2, Section 4.6]. The map α commutes with edge unzips by definition. Cap attachments, cap unzips and the isomorphism φ commute with internal unzips for the same reason as $\wp$, because they are performed at the tangle ends while unzip is internal. This completes the proof. $\qquad\square$

Finally, the following Theorem completes the proof of part Part (3) of the Main Theorem 1.2:

Theorem 3.22. *The map $Z_\xi^w : \widetilde{uTF} \to \mathcal{A}^w$ is the unique homomorphic expansion of $\widetilde{uTF}$, which is compatible with Z^u in the sense of the commutative diagram (2).*

Proof. By Proposition 3.9, Z_ξ^w is compatible with Z^u. By Part (1) (Section 3.1) and Corollary 3.20, $Z_\xi^w = Z_\beta^w$ and uniquely determined by Z^u.

To show that Z_ξ^w is a homomorphic expansion, by Fact 2.6 and Theorem 2.7, one only needs to verify that it satisfies the (R4), Unitarity (U) and Cap (C) equations of Fact 2.6. Of these, $R4$ follows from the fact that Z_ξ^w is a planar algebra map, Theorem 3.17. The Unitarity equation (U) is equivalent to the statement that Z_ξ^w commutes with strand unzips [WKO2, Section 4.3], and hence it is satisfied by Lemma 3.21.

This leaves the Cap Equation, $\qquad\square$

APPENDIX A. THE ALEKSEEV–ENRIQUEZ–TOROSSIAN FORMULA

This appendix is mainly for readers familiar with the Alekseev–Enriquez–Torossian formula for Kashiwara–Vergne solutions in terms of Drinfel'd associators [AET].

There is a linear "interpretation map" (not a map of Lie algebras) $\theta : \mathfrak{lie}_2^2 \to \mathfrak{tder}_2$, sending a pair (a_1, a_2) to the derivation d given by $d(x) = [x, a_1], d(y) = [y, a_2]$. The kernel of this map consists only of pairs of the form $(\alpha x, \beta y)$ for α, β constants. A one-sided inverse $\eta : \mathfrak{tder}_2 \to \mathfrak{lie}_2^2$ which sends a tangential derivation to a pair whose first component

---

[21]In fact, there are further restrictions, eg the two vertices must be of opposite signs, but this is not important for the proof.

has no linear x term and second component has no y term. We denote the exponential of θ by $\Theta : \mathcal{U}(\mathfrak{lie}_2^2)_{exp} \to \mathrm{TAut}_2$. For an element $(e^{\lambda_1}, e^{\lambda_2}) \in \mathcal{U}(\mathfrak{lie}_2^2)_{exp}$, we have $G = \Theta((e^{\lambda_1}, e^{\lambda_2})) \in \mathrm{TAut}_2$ given by $G(x) = e^{-\lambda_1} x e^{\lambda_1}$, and $G(y) = e^{-\lambda_2} y e^{\lambda_2}$. Just as θ is not a Lie algebra map, Θ is not a group homomorphism: composition in TAut_2 is not given by piecewise multiplication of the conjugators. However, θ and Θ present a convenient way to denote tangential derivations and tangential automorphisms as pairs in $\mathfrak{lie}_2^2$ and $(\exp(\mathfrak{lie}_2))^2$, respectively.

Given a Drinfel'd associator Φ, [AET, Theorem 4] gives an explicit formula for a Kashiwara-Vergne solution F as follows[22]:

$$F = (\Phi^{-1}(x, -x - y), e^{-(x+y)/2}\Phi(-x - y, y)e^{y/2}). \tag{13}$$

In other words,

$$F(x) = (\Phi^{-1}(x, -x - y))^{-1} x \Phi^{-1}(x, -x - y),$$

and similarly

$$F(y) = (e^{-(x+y)/2}\Phi(-x - y, y)e^{y/2})^{-1} y e^{-(x+y)/2}\Phi(-x - y, y)e^{y/2}.$$

The point of this Appendix is to show that this formula agrees with our Part (2) of the Main Theorem 1.2, via the correspondences between Drinfel'd associators and expansions Z^u [BN1, Proposition 3.4] and between KV-solutions and expansions Z^w [WKO2, Theorem 4.9].

We first relate $\mathcal{A}^{sw}(\uparrow_2)$ (where V lives) to TAut_2 (where F lives). A Lie word in x and y can be represented by a binary tree with cyclically oriented vertices, and edges oriented towards a single "head": the leaves (tails) are labeled by the letters x and y and the vertices represent brackets. For details see [WKO2, Theorem 3.16] and the discussion following it. There is a *tree attaching* map $l : \mathfrak{tder}_2 \to \mathcal{P}^{sw}(\uparrow_2)$, where $\mathcal{P}^{sw}$ denotes the primitive elements of $\mathcal{A}^{sw}$, as follows. Given $d \in \mathfrak{tder}_2$, we have $\eta(d) = (a_1, a_2) \in (\mathfrak{lie}_2)^2$. Represent the components of $\eta(d)$ by binary trees, and label the heads with x for Lie words coming from a_1, and y for a_2. Then, attach all x-labeled leaves to strand 1, y-labeled leaves to strand 2, and the head of each tree below all tails. The order of tails is irrelevant by the TC relation.

Conversely, elements of $\mathcal{P}^{sw}(\uparrow_2)$ act as tangential derivations on $\mathfrak{lie}_2$ [WKO2, Proposition 3.19]. The action is by adding a third strand and embedding $\mathfrak{lie}_2 \hookrightarrow \mathcal{A}(\uparrow_2)$ as $x \mapsto a_{13}$ and $y \mapsto a_{23}$. Then $\mathcal{P}^{sw}(\uparrow_2)$ embedded in $\mathcal{P}^{sw}(\uparrow_3)$ on the first two strands acts on $\mathfrak{lie}_2$ by the adjoint action (taking commutators). Wheels act trivially, and thus one obtains a homomorphism $\delta : \mathcal{P}^{tree}(\uparrow_2) \to \mathfrak{tder}_2$, whose kernel consists of short arrows on either strand. The map δ is a one-sided inverse to l, namely, $\delta \circ l = \mathrm{Id}_{\mathfrak{tder}_2}$.

Extending δ to exponentials gives a group homomorphism $\Delta : \mathcal{A}^w(\uparrow_2)_{exp} \to \mathrm{TAut}_2$, where $\mathcal{A}^w(\uparrow_2)_{exp}$ denotes the group-like part of $\mathcal{A}^{sw}$. For $D \in \mathcal{A}^w(\uparrow_2)_{exp}$, the map Δ can be described diagrammatically as follows. Add an extra (third) strand, and embed $\mathfrak{lie}_2 \hookrightarrow \mathcal{A}(\uparrow_2)$ as before. Then D, embedded in $\mathcal{A}(\uparrow_3)$ on the first two strands, acts on $\mathfrak{lie}_2$ by conjugation; this defines $\Delta(D)$.

We construct a map L which completes a commutative triangle as in Figure 39. At the level of primitives, the map $l \circ \theta$ has the property that $\delta \circ (l \circ \theta) = \theta$. Extend this to the (completed) enveloping algebra $\hat{\mathcal{U}}(\mathfrak{lie}_2^2)$ as follows. An element of $\hat{\mathcal{U}}(\mathfrak{lie}_2^2)$ is an (infinite) linear

---

[22]There are some notational differences between [AT] and [AET]. There are sign differences between the formula (13) and [AET] due to notational misalignment, for example our Φ is [AET]'s Φ^{-1}. Our notation is consistent with the other papers in this series and the formulas are computationally verified in [WKO4].

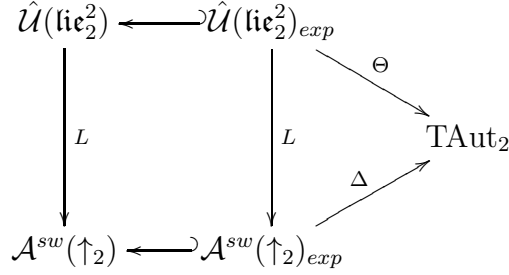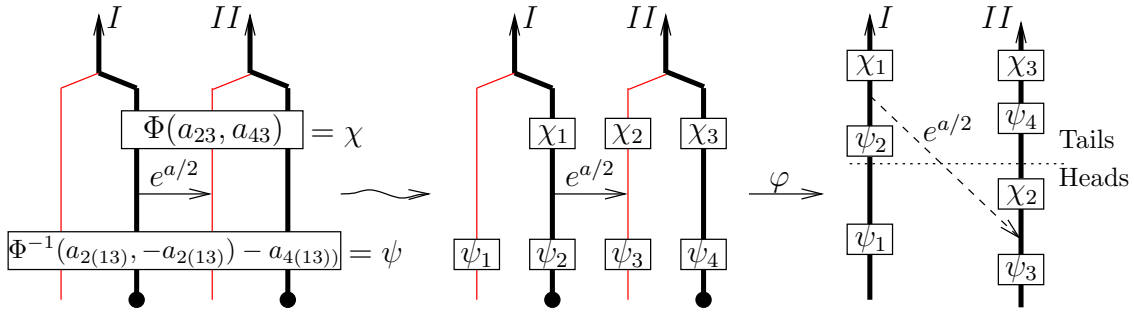**Figure 39.** The connection between $\mathcal{A}^{sw}(\uparrow_2)$ and TAut_2.

Figure 40. To compute $\varphi(\Phi^{-1}(a_{2(13)}, -a_{2(13)} - a_{4(13)}) \cdot e^{a_{23}/2} \cdot \Phi(a_{23}, a_{43}))$ we switch to a *placement notation* in which we mark on each skeleton strand the elements that have arrows ending on it. For this purpose we denote $\Phi^{-1}(a_{2(13)}, -a_{2(13)} - a_{4(13)}) =: \psi$ and $\Phi(a_{23}, a_{43}) =: \chi$.

combination of products of Lie words. As with l, represent each Lie word as a labeled tree, but then attach the products of these labeled trees to the two strands by attaching *all heads* below *all tails*. The order of tails doesn't matter, the order of heads is in the order in which the words are multiplied. Call this map L, and note that L is *not* an algebra homomorphism: it does not respect multiplication in $\hat{\mathcal{U}}(\mathfrak{lie}_2^2)$. However, the restriction of L to the group-like part $\hat{\mathcal{U}}(\mathfrak{lie}_2^2)_{exp}$, also denoted L fits into a commutative triangle $\Theta = \Delta \circ L$. Note that $L \neq e^l$.

Let Z^u be an expansion of *sKTG* given by the Drinfel'd associator Φ. Let V be the Z^w-value of the vertex for the unique homomorphic expansion Z^w compatible with Z^u. Then $F = \Delta(V)$ is a solution to the Kashiwara-Vergne problem [WKO2]. Our goal is to relate the Θ-image of the [AET] formula $\Theta(\Phi^{-1}(x, -x-y), e^{-(x+y)/2}\Phi(-x-y, y)e^{y/2})$ to $\Delta(V)$. Note that wheels are in the kernel of Δ and the [AET] formula only concerns the *tree* component V^{tree}.

The accomplish this, we need to compute $V^{tree} = \varphi(\Phi^{-1}(a_{2(13)}, -a_{2(13)} - a_{4(13)}) \cdot e^{a_{23}/2} \cdot \Phi(a_{23}, a_{43}))$ more explicitly, as shown in Figure 40, and explained in the caption. The first strand of $\mathcal{A}^{sw}(\uparrow_2)$ joins strands 1 and 2 in a vertex, and the second strand of $\mathcal{A}^w(\uparrow_2)$ joins strands 3 and 4. Strands 1 and 3 are punctured and strands 2 and 4 are capped. Let us call the two strands of $\mathcal{A}^w(\uparrow_2)$ strand I and strand II to avoid confusion. Recall from the construction of φ that one first slides arrow tails from the capped strands "up" through the vertices, then slides all the heads up from the punctured strands 1 and 3. Thus one obtains an element of $\mathcal{A}^w(\uparrow_2)$ in which all arrow heads are below all tails on both strands.
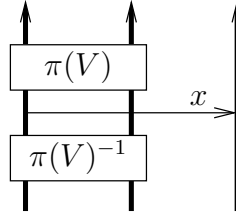
44

Figure 41. The action of $\pi(V)$ on the generator x of $\mathfrak{lie}_2$.
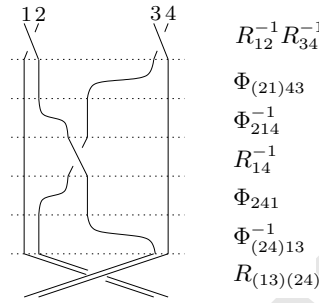

Figure 42. A different expression of β^b.

Now we are ready to compute how $\pi(V) \in \mathcal{A}^w(\uparrow_2)$ acts on the generator x of $\mathfrak{lie}_2$ and match this to the formula 13. Recall the value of $\pi(V)$ shown in Figure 40. The generator x is represented by an arrow from the first strand to the added third strand, and the action is by conjugation, as shown in Figure 41. To compute this, one commutes the tail of x to the top of the strand across $\pi(V)$ using $\overrightarrow{STU}$ relations, thereby $\pi(V)$ and $\pi(V)^{-1}$ cancel, and the result of the action remains. Observe that due to the TC relation, only arrows with heads on strand I act nontrivially on x, in other words only ψ_1 matters, which came from $\Phi^{-1}(a_{2(13)}, -a_{2(13)} - a_{4(13)})$. The arrows a_{23} and a_{43} act trivially on x, so, more simply stated, the action on x is by $\varphi(\Phi^{-1}(a_{21}, -a_{21} - a_{41}))$. Note that $L(\Phi^{-1}(x, -x - y), 0) = \varphi(\Phi^{-1}(a_{21}, -a_{21} - a_{41}))$, so Theorem 1.2 agrees with Formula (13) in the first component.

One can proceed similarly for the second component: the action on y is by

$$\varphi(\Phi^{-1}(a_{23}, -a_{23} - a_{43})e^{a_{23}}\Phi(a_{23}, a_{43})) = L(0, \Phi^{-1}(x, -x - y)e^{x/2}\Phi(x, y)).$$

While this does not match the second component of Formula (13), it only differs from it by a hexagon relation. Alternatively, note that one can obtain the second component of the Formula (13) "on the nose" by starting from an equivalent (isotopic) expression[23] of β^b, as shown in Figure 42. This completes the proof. □

A sequel paper [WKO4] verifies the results in this appendix by explicit computations in low degrees.

References

[AET]   A. Alekseev, B. Enriquez, and C. Torossian, *Drinfeld's associators, braid groups and an explicit solution of the Kashiwara-Vergne equations,* Publications Mathématiques de L'IHÉS, **112-1** (2010) 143–189, arXiv:0903.4067.

---

[23]We thank Karene Chu for this idea.

45

[AKKN1] A. Alekseev, N. Kazumi, Y. Kuno, F. Naef, *The Goldman-Turaev Lie bialgebra in genus zero and the Kashiwara–Vergne problem,* arXiv:1703.05813.

[AKKN2] A. Alekseev, N. Kazumi, Y. Kuno, F. Naef, *Goldman-Turaev formality implies Kashiwara–Vergne,* Quantum Topology **11-4** (2020) 657–689.

[AM] A. Alekseev and E. Meinrenken, *On the Kashiwara-Vergne conjecture,* Inventiones Mathematicae, **164** (2006) 615–634, arXiv:0506499.

[AN] A. Alekseev, F. Naef, *Goldman-Turaev formality from the Knizhnik-Zamolodchikov connection* Comptes Rendus Mathematique **355-11** (2017) 1138–1147

[AT] A. Alekseev and C. Torossian, *The Kashiwara-Vergne conjecture and Drinfeld's associators,* Annals of Mathematics **175** (2012) 415–463, arXiv:0802.4300.

[BN1] D. Bar-Natan, *On associators and the Grothendieck-Teichmuller Group I,* in *Selecta Mathematica,* New Series **4**, 183–212, June 1996.

[BN2] D. Bar-Natan, *Non-associative tangles,* in *Geometric topology* (proceedings of the Georgia international topology conference), (W. H. Kazez, ed.), 139–183, Amer. Math. Soc. and International Press, Providence, 1997.

[BND1] D. Bar-Natan and Z. Dancso, *Homomorphic expansions for knotted trivalent graphs*, Journal of Knot Theory and its Ramifications Vol. **22**, No. 1 (2013) arXiv:1103.1896

[BDS] D. Bar-Natan, Z. Dancso and N. Scherich, *Ribbon 2-Knots, $1 + 1 = 2$, and Duflo's Theorem for Arbitrary Lie Algebras,* Algebraic and Geometric Topology **20** 7 (2020) 3733–3760 arXiv:1811.08558

[BDV] D. Bar-Natan, Z. Dancso and R. van der Veen, *Over then Under Tangles* To appear in the Special Issue in memory of Vaughan Jones, Journal of Knot Theory and its Ramifications. arXiv:2007.09828

[BGRT] D. Bar-Natan, S. Garoufalidis, L. Rozansky and D. P. Thurston, *Wheels, wheeling, and the Kontsevich integral of the unknot,* Israel Journal of Mathematics **119** (2000) 217–237, arXiv:q-alg/9703025.

[BLT] D. Bar-Natan, T. Q. T. Le, and D. P. Thurston, *Two applications of elementary knot theory to Lie algebras and Vassiliev invariants,* Geometry and Topology **7-1** (2003) 1–31, arXiv:math.QA/0204311.

[Da] Z. Dancso, *On a Kontsevich Integral for Knotted Trivalent Graphs,* Algebraic and Geometric Topology **10** (2010) 1317–1365, arXiv:0811.4615.

[DHR1] Z. Dancso, I. Halacheva, M. Robertson *Circuit Algebras are Wheeled Props* Journal of Pure and Applied Algebra **225-12** (2021)106767

[DHR2] Z. Dancso, I. Halacheva, M. Robertson *A Topological characterisation of the Kashiwara-Vergne Groups,* Transactions of the American Mathematical Society **376**-5 (2023) 3265–3317 arXiv:2106.02373

[DHoR] Z. Dancso, T. Hogan, M. Robertson, *A diagrammatic description of the Alekseev-Torossian map,* arXiv:2211.11370.

[Dr] V. G. Drinfel'd, *Quasi-Hopf Algebras,* Leningrad Math. J. **1** (1990) 1419–1457.

[J] V. F. R. Jones, *Planar Algebras I* arXiv:math/9909027, to appear in *New Zeland J. Math.*

[KV] M. Kashiwara and M. Vergne, *The Campbell-Hausdorff Formula and Invariant Hyperfunctions,* Invent. Math. **47** (1978) 249–272.

[LM] T. Q. T. Le and J. Murakami, *The universal Vassiliev-Kontsevich invariant for framed oriented links,* Compositio Math. **102** (1996) 41–64, arXiv:hep-th/9401016.

[M] Gwénaël Massuyeau *Formal descriptions of Turaev's loop operations* Quantum Topology **9-1** (2018) 39–117.

[T] D. P. Thurston *The Algebra of Knotted Trivalent Graphs and Turaev's Shadow World* Invariants of Knots and 3-manifolds (Kyoto 2001), Geometry Topology Monographs **4** 337–362, arXiv:math.GT/0311458

[WKO0] D. Bar-Natan and Z. Dancso, *Finite Type Invariants of W-Knotted Objects: From Alexander to Kashiwara and Vergne*, paper, videos (wClips) and related files at http://www.math.toronto.edu/~drorbn/papers/WKO/. The arXiv:1309.7155 edition may be older.

[WKO1] D. Bar-Natan and Z. Dancso, *Finite Type Invariants of W-Knotted Objects I: W-Knots and the Alexander Polynomial*, Alg. Geom. Topology **16** (2016) 1063–1133. arXiv:1405.1956

[WKO2C] D. Bar-Natan and Z. Dancso, *Corrigendum to "Finite Type Invariants of W-Knotted objects II"* to appear in Math. Annalen; Edited full paper available at: arXiv:1405.1955

ancso:WKO2 | [WKO2] D. Bar-Natan and Z. Dancso, *Finite Type Invariants of W-Knotted objects II: Tangles, Foams and the Kashiwara-Vergne Problem* Math. Annalen **367** (2017) 1517–1586. Section references point to v4 of arXiv:1405.1955.

DoubleTree | [WKO3] D. Bar-Natan and Z. Dancso, *Finite Type Invariants of w-Knotted Objects III: From Associators to Solutions of the Kashiwara-Vergne problem* (self-reference), paper and related files at http://www.math.toronto.edu/~drorbn/papers/DoubleTree/. The arXiv:????.???? edition may be older.

Natan:WKO4 | [WKO4] D. Bar-Natan, *Finite Type Invariants of w-Knotted Objects IV: Some Computations* arXiv:1511.05624

DEPARTMENT OF MATHEMATICS, UNIVERSITY OF TORONTO, TORONTO ONTARIO M5S 2E4, CANADA
Email address: drorbn@math.toronto.edu
URL: http://www.math.toronto.edu/~drorbn

SCHOOL OF MATHEMATICS AND STATISTICS, THE UNIVERSITY OF SYDNEY, CARSLAW BUILDING, CAMPERDOWN, NSW, AUSTRALIA
Email address: zsuzsanna.dancso@anu.edu.au
URL: http://www.math.toronto.edu/zsuzsi